Amiloride inhibits macropinocytosis by lowering submembranous pH and preventing Rac1 and Cdc42 signaling

Mirkka Koivusalo,[1] Christopher Welch,[2] Hisayoshi Hayashi,[1,3] Cameron C. Scott,[1,4] Moshe Kim,[1] Todd Alexander,[1,5] Nicolas Touret,[1,6] Klaus M. Hahn,[2] and Sergio Grinstein[1]

[1]Cell Biology Program, The Hospital for Sick Children, Toronto, Ontario M5G 1X8, Canada
[2]Department of Pharmacology, University of North Carolina at Chapel Hill, Chapel Hill, NC 27599
[3]Laboratory of Physiology, School of Food and Nutritional Sciences, University of Shizuoka, Yada 52-1, Suruga-ku, Shizuoka 422-8526, Japan
[4]Department of Biochemistry, University of Geneva - Sciences II 30, CH-1211 Geneva, Switzerland
[5]Department of Pediatrics and Physiology and [6]Department of Biochemistry, University of Alberta, Edmonton, Alberta T6G 2H7, Canada

Macropinocytosis is differentiated from other types of endocytosis by its unique susceptibility to inhibitors of Na^+/H^+ exchange. Yet, the functional relationship between Na^+/H^+ exchange and macropinosome formation remains obscure. In A431 cells, stimulation by EGF simultaneously activated macropinocytosis and Na^+/H^+ exchange, elevating cytosolic pH and stimulating Na^+ influx. Remarkably, although inhibition of Na^+/H^+ exchange by amiloride or HOE-694 obliterated macropinocytosis, neither cytosolic alkalinization nor Na^+ influx were required. Instead, using novel probes of submembranous pH, we detected the accumulation of metabolically generated acid at sites of macropinocytosis, an effect counteracted by Na^+/H^+ exchange and greatly magnified when amiloride or HOE-694 were present. The acidification observed in the presence of the inhibitors did not alter receptor engagement or phosphorylation, nor did it significantly depress phosphatidylinositol-3-kinase stimulation. However, activation of the GTPases that promote actin remodelling was found to be exquisitely sensitive to the submembranous pH. This sensitivity confers to macropinocytosis its unique susceptibility to inhibitors of Na^+/H^+ exchange.

Introduction

Macropinocytosis is the most effective way for cells to ingest large amounts of extracellular fluid. In some cell types macropinocytosis is a constitutive process: immature dendritic cells use it to sample soluble antigens (Sallusto et al., 1995) and *Dictyostelium* amoeba for nutrient uptake (Cardelli, 2001). Constitutive macropinocytosis is also observed in fibroblasts transformed with oncogenic v-Src or K-Ras (Amyere et al., 2000, 2002). Alternatively, macropinocytosis can be transiently induced by growth factors, such as epidermal growth factor or macrophage colony–stimulating factor (Racoosin and Swanson, 1989; West et al. 2000).

Correspondence to Sergio Grinstein: sga@sickkids.ca

Abbreviations used in this paper: CRIB, Cdc42/Rac-interacting binding; DIC, differential interference contrast; FBE, free barbed end; GEF, guanine nucleotide exchange factor; Grb2, growth factor receptor-bound protein 2; HOE-694, (3-methylsulphonyl-4-piperidinobenzoyl)guanidine methanesulphonate; NHE, Na^+/H^+ exchanger; NMG, *N*-methylglucamine; PAK, p21-activated kinase; PBD, p21-binding domain of PAK; PI3K, phosphatidylinositol-3-kinase; PIP_3, phosphatidylinositol-(3,4,5)-trisphosphate; pH_c, cytosolic pH; pH_{sm}, submembranous pH; SNARF-5F, seminaphthorhodafluor dye-5; SEpHluorin, SuperEcliptic pHluorin; TMR, tetramethylrhodamine.

The remodelling of the cytoskeleton that leads to macropinocytosis requires phosphatidylinositol-3-kinase (PI3K) activity at the plasma membrane (Araki et al., 1996; Rupper et al., 2001; Lindmo and Stenmark, 2006). Although the entire signaling sequence is incompletely understood, the GTPases Rac1 (West et al., 2000) and Cdc42 (Garrett et al., 2000), as well as p21-activated kinase 1 (PAK1; Dharmawardhane et al., 2000), are involved in actin polymerization, and CtBP1/BARS is required for macropinosome closure (Liberali et al., 2008). The activation of PI3K and the engagement of Rho family GTPases are common to a variety of actin-dependent processes such as phagocytosis and chemotaxis. Thus, treatment with inhibitors like wortmannin and *Clostridium difficile* toxin B effectively blocks these processes, as well as

The Rockefeller University Press $30.00
J. Cell Biol. Vol. 188 No. 4 547–563
www.jcb.org/cgi/doi/10.1083/jcb.200908086

macropinocytosis. In contrast, macropinosome formation appears to be uniquely susceptible to inhibition by amiloride and its analogues, and this property has been extensively used as an identifying feature of macropinocytosis (West et al., 1989; Veithen et al., 1996; Meier et al., 2002). Amiloride, a guanidinium-containing pyrazine derivative, has been used extensively as an inhibitor of Na^+/H^+ exchangers (NHEs; Grinstein et al., 1989; Orlowski and Grinstein, 2004). However, amiloride is not a universal nor a specific inhibitor of NHE: the affinity of the different NHE isoforms for amiloride varies greatly and, importantly, the drug also inhibits conductive Na^+ channels and Na^+/Ca^{2+} exchangers (Alvarez de la Rosa et al., 2000; Masereel et al., 2003). To increase the potency and selectivity of NHE inhibitors several amiloride analogues have been synthesized, including ethylisopropylamiloride (EIPA; Masereel et al., 2003) and (3-methylsulphonyl-4-piperidinobenzoyl)guanidine methanesulphonate (HOE-694), which is specific for the NHE1 isoform (Counillon et al., 1993).

How amiloride inhibits macropinocytosis remains unknown. To the extent that EIPA also blocks macropinocytosis, NHEs are likely to play a role in the process (Cosson et al., 1989; West et al., 1989), but the mechanism linking ion exchange and vacuole formation is not apparent. Three possible mechanisms can be contemplated: (1) uptake of Na^+ by the exchangers may increase the intracellular solute concentration, driving osmotically obliged water and causing swelling that would favor the protrusion of macropinocytic pseudopods. Though the stoichiometric exchange of Na^+ for H^+ is osmotically neutral, extruded H^+ are replaced from intracellular buffers, resulting in a net osmotic gain; (2) NHE could be acting indirectly by altering the cytosolic concentration of calcium, which has been suggested to regulate macropinocytosis (Falcone et al., 2006). Na^+ delivered intracellularly in exchange for H^+ can promote the uptake of calcium via Na^+/Ca^{2+} exchange; (3) the effect of NHE on macropinocytosis may be mediated by changes in cytosolic pH. Stimulation of NHE by hormones or growth promoters has been shown to alkalinize the cytosol (Rothenberg et al., 1983; L'Allemain et al., 1984; Grinstein et al., 1985; Van Obberghen-Schilling et al., 1985). Conversely, inhibition of the antiporters impairs the ability of cells to eliminate H^+ generated metabolically and can cause acidification (L'Allemain et al., 1984, 1985; Grinstein et al., 1985; Liaw et al., 1998). The changes in pH resulting from modulation of NHE activity could conceivably alter the signaling and/or cytoskeleton rearrangements required for macropinocytosis.

We investigated the functional relationship between macropinocytosis and Na^+/H^+ exchange. Macropinocytosis was induced in A431 cells by EGF, and NHE activity was modulated pharmacologically and by ion substitution. Moreover, we measured the bulk cytosolic pH and the pH of the inner aspect of the plasma membrane during the course of macropinocytosis. Our results indicate that NHE1 activity is required to attain a critical H^+ concentration in the immediate vicinity of the plasma membrane that promotes actin polymerization during macropinocytosis.

Results

Inhibition of macropinocytosis by NHE antagonists

A431 cells, which have been used extensively to study macropinocytosis, were chosen to investigate the mechanism of action of amiloride and its analogues. As reported previously (West et al., 1989; Araki et al., 2007; Liberali et al., 2008), addition of EGF to serum-depleted A431 cells led to extensive membrane ruffling and uptake of extracellular medium, visualized as trapping of the fluid-phase marker tetramethylrhodamine (TMR)-dextran (Fig. 1 A). The ruffling, which was apparent by differential interference contrast (DIC) microscopy (Video 1), was associated with extensive actin recruitment, revealed by staining with labeled phalloidin. These effects were most noticeable in the cells at the periphery of the subconfluent islands (Fig. 1 A). The increases in fluid phase uptake and actin polymerization were obliterated by pretreatment with either latrunculin B or with the PI3K inhibitor LY294002, consistent with mediation by macropinocytosis (Fig. 1 A).

As illustrated in Fig. 1 A, the prototypical NHE inhibitor amiloride effectively inhibited EGF-induced fluid phase uptake and actin polymerization. Because at the concentrations used to inhibit Na^+/H^+ exchange amiloride has been reported to affect several other pathways (Alvarez de la Rosa et al., 2000; Masereel et al., 2003), we also tested HOE-694, a more selective NHE antagonist. As shown in Fig. 1, A and B, 10 µM HOE-694 greatly depressed macropinocytic activity. Parallel experiments verified that, at this concentration, HOE-694 eliminated Na^+/H^+ exchange. NHE activity was measured as the rate of Na^+-induced recovery of the cytosolic pH (pH_c) from an acid load. Ratiometric determinations of pH_c using seminaphthorhodafluor dye-5 (SNARF-5F) demonstrated that when Na^+ was reintroduced to the medium the cells recovered rapidly from a cytosolic acidification imposed by an ammonium prepulse. In the presence of 10 µM HOE-694, however, this response was completely eliminated (Fig. 1 C). At the submicromolar doses found to inhibit exchange in A431 cells (Fig. 1 D) HOE-694 selectively inhibits NHE1, with negligible effects on other isoforms (Counillon et al., 1993). Fig. 1, C and D therefore suggest that NHE1 is the main, if not the sole isoform active in the plasma membrane of A431 cells. For this reason, and to minimize off-target effects, HOE-694 was the inhibitor of choice in subsequent experiments.

Changes in pH_c during macropinocytosis

EGF is known to stimulate Na^+/H^+ exchange and is capable of elevating pH_c (Moolenaar et al., 1983; Rothenberg et al., 1983; Yanaka et al., 2002). The resulting alkalinization has been implicated in the initiation of the proliferative effects of EGF (L'Allemain et al., 1984; L'Allemain and Pouyssegur, 1986) and may similarly be required for macropinocytosis. This notion was tested by measuring the pH_c changes elicited by the growth factor in the presence and absence of HOE-694. As shown in Fig. 2 A, A431 cells stimulated with EGF underwent a rapid and sizable (≥0.3 unit) alkalinization. In contrast, a net

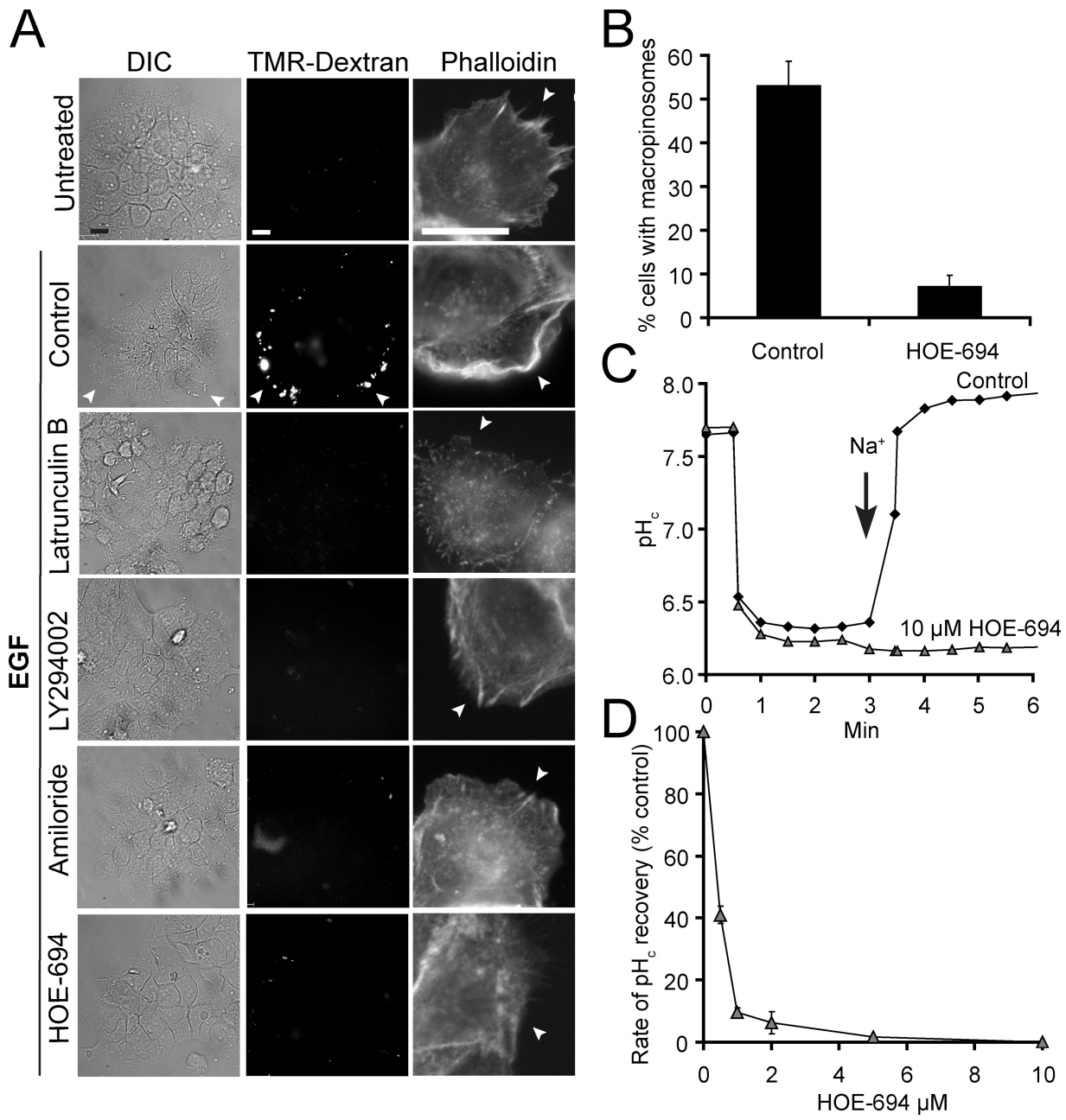

Figure 1. **Effect of inhibitors on macropinocytosis and NHE activity.** (A) DIC (left) and TMR-dextran epifluorescence images (middle) of islands of A431 cells incubated in the absence (Untreated) or presence of EGF as detailed in Materials and methods. Arrowheads point to dextran-filled macropinosomes. After determination of macropinocytosis, cells were fixed and stained with rhodamine-phalloidin to visualize actin (left). Arrowheads point to the aspect of the cell not in contact with neighboring cells. Bar, 10 μm. (B) Quantification of macropinocytosis in control and HOE-694-treated cells. Data are means ± SE of ≥5 separate experiments. (C) Effect of 10 μM HOE-694 on Na^+-induced recovery of pH_c after an acid load. NHE activity initiated where indicated by reintroduction of Na^+. Results are representative of 3–4 similar experiments. (D) Concentration dependence of the effect of HOE-694. NHE activity was measured as in C and rates were calculated from the slopes from Na^+-induced pH_c recovery curves. Data are means ± SE of three experiments. Where missing, error bars are smaller than symbol.

acidification was observed when cells were treated with EGF in the presence of maximally inhibitory doses of HOE-694. The rapid acidification likely results from the generation of acid equivalents by metabolic pathways stimulated by the growth factor. This burst of acid generation is normally not apparent because it is outstripped by the vigorous H^+ extrusion mediated by Na^+/H^+ exchange and is only detectable when unmasked by inhibition of NHE1.

Measurements of the bulk cytosolic pH, such as those described above using SNARF-5F, may not accurately reflect the H^+ concentration in the vicinity of the membrane where the receptors become activated and ruffling is initiated. To more precisely determine the submembranous pH (pH_{sm}) we generated a genetically encoded ratiometric pH probe, shown schematically in Fig. 2 B, which was targeted to the inner aspect of plasmalemma. When expressed in A431 cells the Lyn-SuperEcliptic (SE)

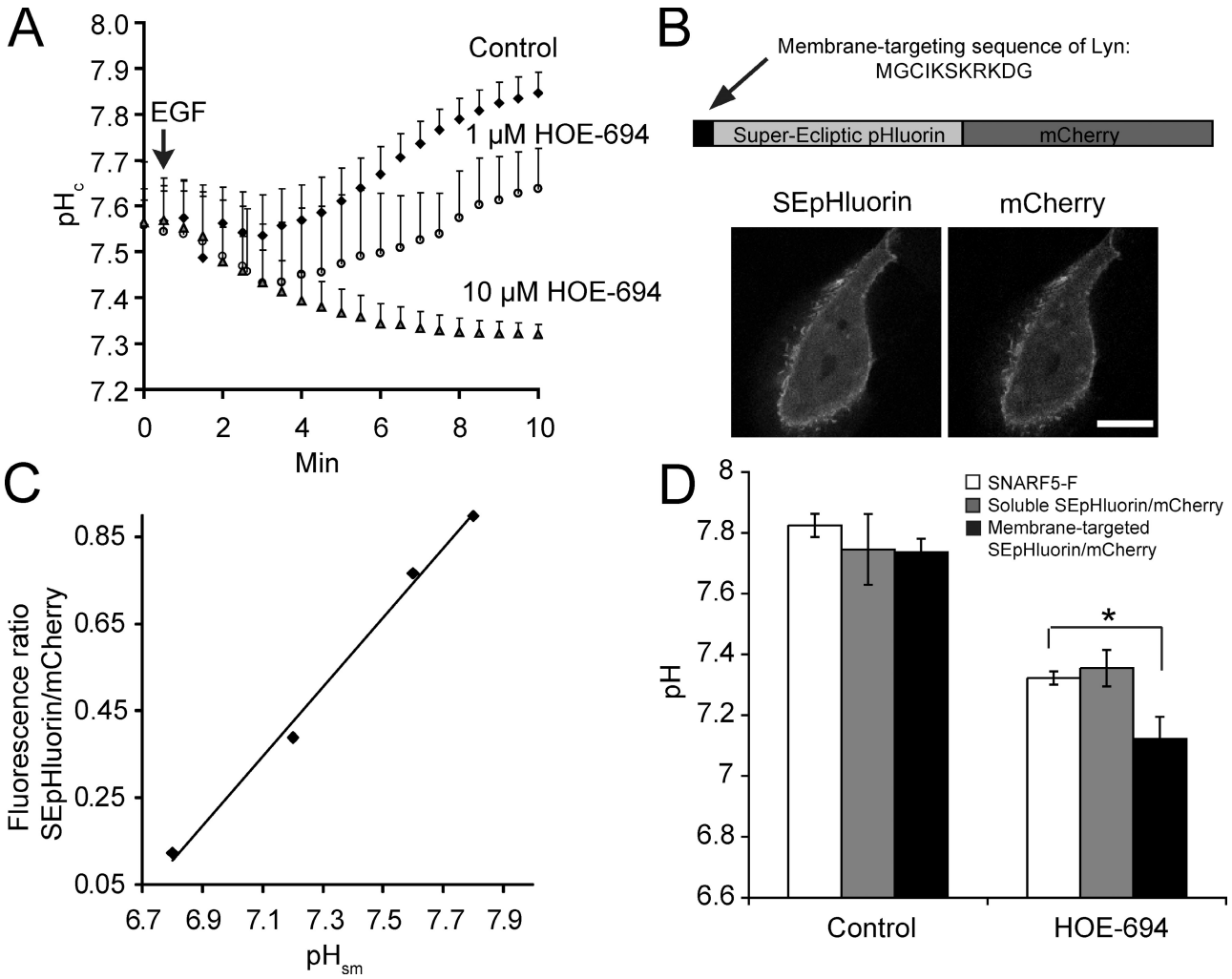

Figure 2. **Effect of HOE-694 on EGF-induced changes in pH.** (A) SNARF-5F fluorescence ratio measurement of pH_c. Where indicated by arrow A431 cells were stimulated with EGF in the absence (Control) or presence of HOE-694. Data are means ± SE of 3–6 experiments. (B) Top: schematic of the structure of membrane-targeted SEpHluorin/mCherry chimaera used to measure pH_{sm}. Bottom: confocal images of SEpHluorin (left) and mCherry fluorescence (right) in A431 cells. Bar, 10 µm. (C) Representative pH_{sm} calibration curve. Cells transfected with membrane-targeted SEpHluorin/mCherry were incubated in the presence of K^+/nigericin buffers of predetermined pH. Fluorescence intensities were measured and the ratio of SEpHluorin/mCherry fluorescence is plotted as a function of pH. (D) Comparison of pH_c (SNARF5-F and soluble SEpHluorin/mCherry) vs. pH_{sm} (membrane-targeted SEpHluorin/mCherry) in cells treated with EGF for 10 min in Na^+ medium in the presence and absence of HOE-694 (10 µM). Data are means ± SE of 3–5 experiments. *, $P < 0.05$.

pHluorin/mCherry probe was found predominantly at the plasma membrane (Fig. 2 B). That the chimera is a suitable indicator of pH was verified by in situ calibrations using ionophores to clamp the intracellular pH (see Materials and methods); the SEpHluorin to mCherry fluorescence ratio varied nearly linearly with pH in the 6.8–7.8 range (Fig. 2 C), in accordance with the $pK_a = 7.2$ reported for SEpHluorin (Sankaranarayanan et al., 2000).

Next, we examined the effect of EGF and of maximally inhibitory concentrations of HOE-694 on pH_{sm}. Although the overall pattern of responsiveness was similar, the changes reported by the submembranous chimera were more profound: whereas in stimulated cells the NHE inhibitor produced a net pH_c decrease of 0.5 pH units, pH_{sm} dropped by as much as 0.7 pH units (Fig. 2 D). A soluble form of the SEpHluorin/mCherry probe lacking the membrane-targeting domain yielded results that were similar to those obtained with SNARF-5F (Fig. 2 D), implying that the larger response detected by Lyn-SEpHluorin/mCherry is a valid measure of the localized accumulation of H^+ in the submembranous space. Together, these measurements not only confirm the burst of metabolic acid generation, but in addition reveal that its effects are more pronounced in the immediate vicinity of the membrane, where macropinocytic lamellipodia extend.

Macropinocytosis under Na^+-free conditions

To confirm that amiloride and HOE-694 inhibit macropinocytosis by impairing Na^+/H^+ exchange, we performed experiments in media devoid of Na^+. As shown in Fig. 3, A–C, omission of Na^+ resulted in a drastic reduction in macropinocytic efficiency, in accordance with previous findings (West et al., 1989), regardless of whether the substituent was K^+ or *N*-methylglucamine (NMG^+). Neither of these cations is transported by NHE1 and, as a result, the alkalinization induced by EGF in physiological media is absent when Na^+ is omitted (Fig. 3 C). Instead, a sharp acidification is recorded, resembling the effects of maximal doses of HOE-694 (Figs. 2 A and 3 C).

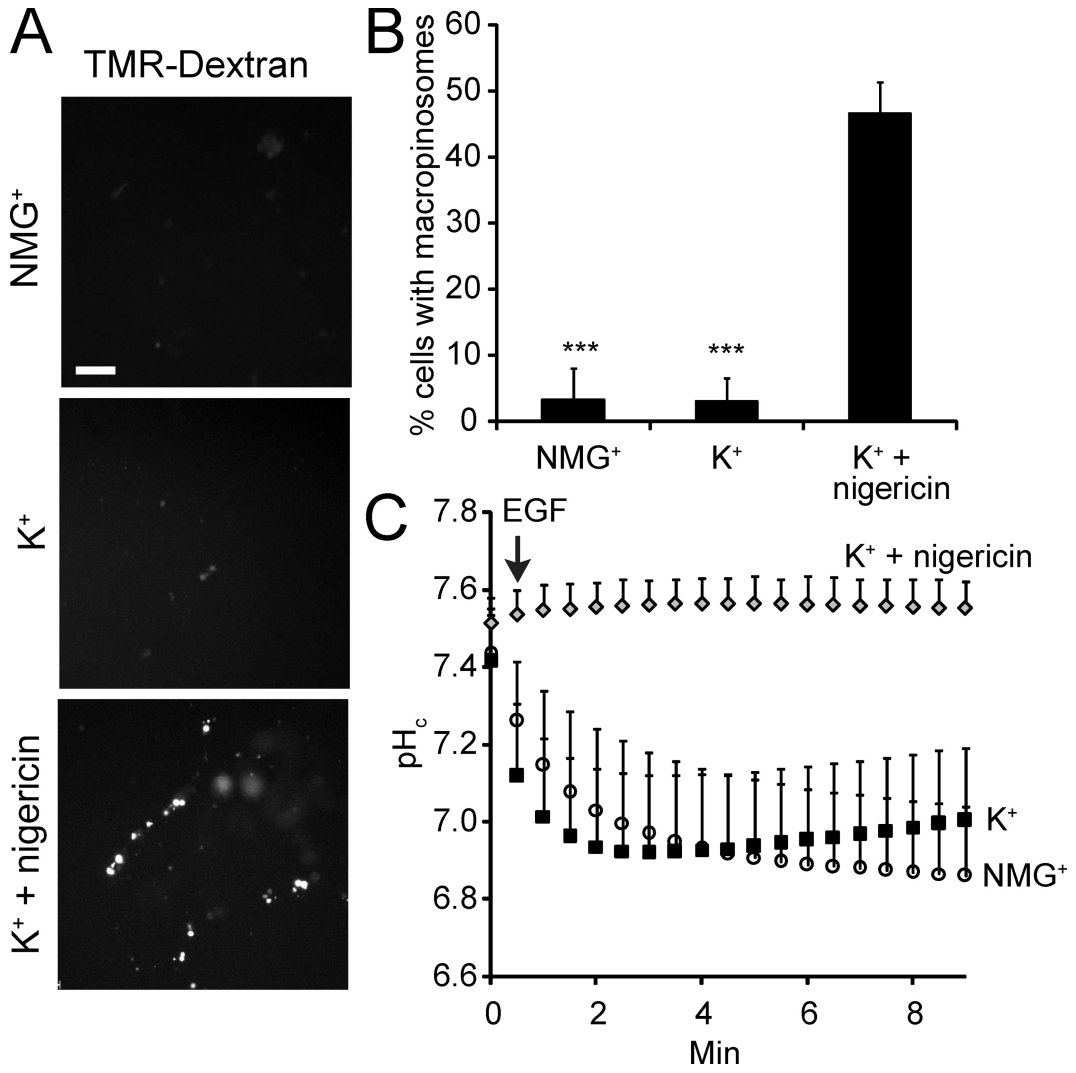

Figure 3. **Effect of Na^+ omission on macropinocytosis and pH_c.** (A) Epifluorescence images of islands of A431 cells after 10 min incubation with TMR-dextran and EGF in the indicated Na^+-free media. To clamp pH_c (bottom panel), cells were preincubated in K^+/nigericin. Bar = 10 µm. (B) Quantification of macropinocytosis in Na^+-free solutions. Data are means ± SE of 3–4 experiments. Data were compared with controls in Na^+-rich medium (as in Fig. 1 B) and significance calculated using Student's *t* test; ***, $P < 0.001$. (C) Measurement of pH_c using SNARF-5F in cells treated with EGF in the indicated buffers. Data are means ± SE of three experiments, each measuring 10 cells.

The preceding experiments confirm that Na^+/H^+ exchange is required for macropinocytosis, but these and previous data (Cosson et al., 1989; West et al., 1989) cannot define whether entry of Na^+ or extrusion of H^+ is the critical event. This was addressed using nigericin, an electroneutral K^+/H^+ exchanger. As shown in Fig. 3 C, when added in the presence of 140 mM extracellular K^+ to balance the osmolarity when omitting Na^+, the ionophore effectively neutralized the metabolic acidification triggered by EGF. Importantly, the ability of EGF to induce TMR-dextran uptake was restored by nigericin, implying that extrusion of H^+, and not the entry of Na^+, per se, is the key requirement for macropinosome formation.

The experiments in Fig. 3 also imply that the alkalinization mediated by NHE1 that normally accompanies stimulation by EGF is not absolutely required for macropinocytosis because the latter persists when pH_c is clamped with nigericin/K^+. Instead, it is more likely that NHE activity is required to prevent the development of an acidification that may be deleterious to macropinocytosis.

pH dependence of macropinocytosis

The preceding experiments suggested that, in the absence of Na^+/H^+ exchange, macropinocytosis may be impaired by the accumulation of H^+ (equivalents) generated metabolically after engagement of EGF receptors. To validate this notion we measured the intracellular pH dependence of macropinocytosis. The uptake of TMR-dextran in response to EGF was quantified in cells where pH_c was clamped at the desired level using nigericin/K^+ (Fig. 4). Maintaining pH at a level comparable to that attained when cells are stimulated in physiological media enabled the cells to respond to EGF with robust macropinocytosis, despite the absence of Na^+. Normal macropinocytosis was also observed when pH_c was clamped near the resting level recorded in unstimulated cells (7.5–7.6). Remarkably, TMR-dextran uptake

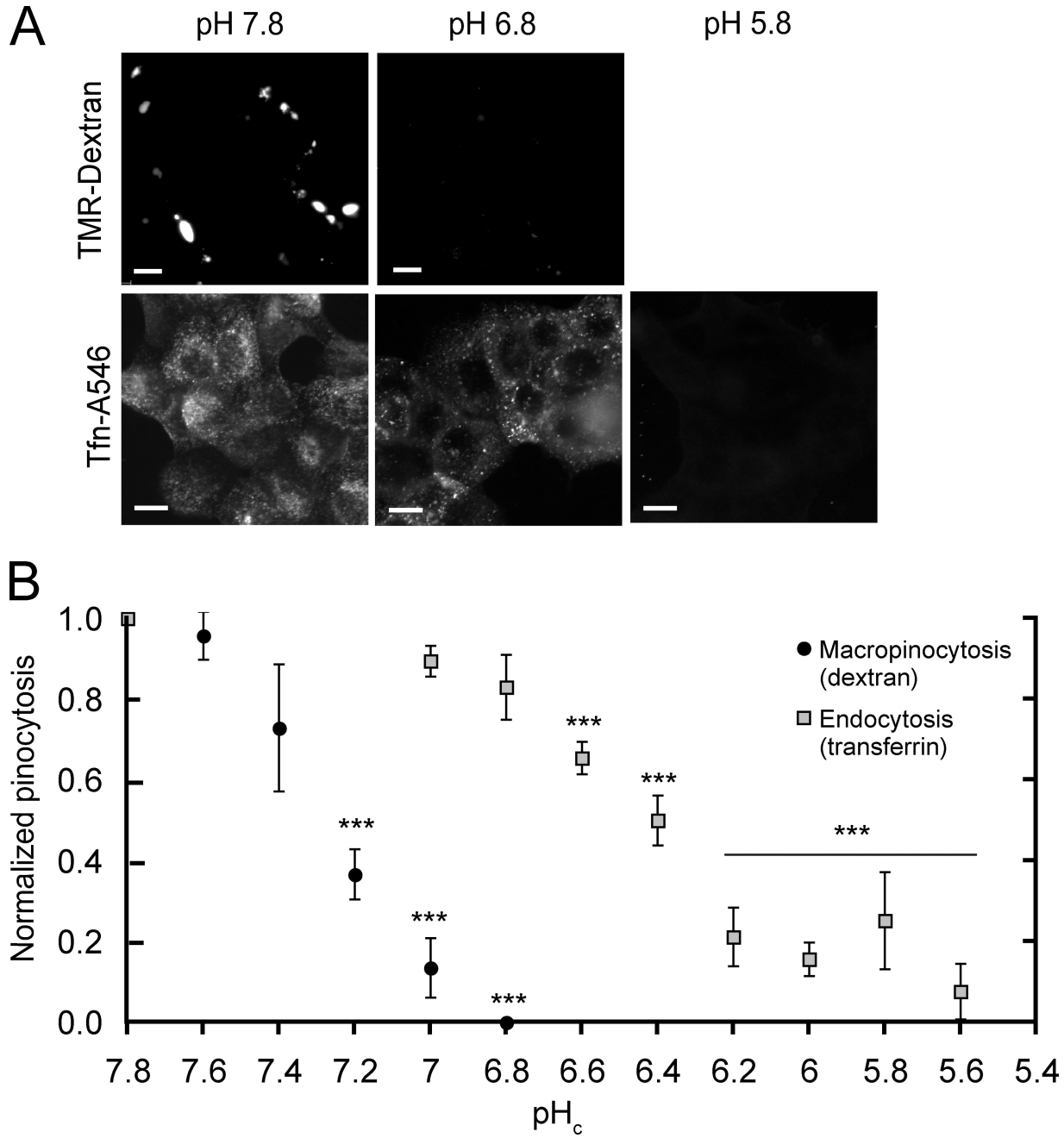

Figure 4. **Measurement of macropinocytosis and endocytosis in pH$_c$-clamped cells.** (A) The cytosolic pH of A431 cells was clamped at 7.8 or 6.8 with K^+/nigericin and TMR-dextran and EGF were added to measure macropinocytosis. After washing, red fluorescence images were acquired. To measure endocytosis, cells were pH$_c$-clamped, incubated with Tfn-A546 for 15 min, acid-washed, fixed, and imaged. Bar, 10 µm. (B) Effect of pH on macropinocytosis and on clathrin-mediated endocytosis. Cells were subjected to pH$_c$ clamping and macropinocytosis quantified as in Fig. 1; clathrin-mediated endocytosis was assessed as Tfn-A546 uptake. Data are means ± SE of 3–4 experiments. Data were normalized to pH$_c$ 7.8 and the significance of the differences calculated using Student's *t* test comparing values within a dataset to pH$_c$ 7.8; ***, $P < 0.001$.

dropped acutely as pH$_c$ was decreased progressively. Even comparatively modest changes in pH produced marked, highly significant decreases in macropinocytic efficiency (Fig. 4 B) and virtually complete inhibition was noted at pH 6.8 (Fig. 4, A and B). Of note, when pH$_c$ was clamped at physiological values the presence of 10 µM HOE-694 was without effect on macropinocytosis (not depicted). This rules out off-target effects of the inhibitor and confirms that pH maintenance, rather than NHE activity itself or the associated Na^+ gain, is required for macropinocytosis.

In contrast to the exquisite sensitivity of macropinocytosis to acidification, clathrin-mediated endocytosis was virtually unaffected by modest changes in pH$_c$ and was inhibited only after marked cytosolic acidification (Fig. 4, A and B). This was determined by measuring the uptake of Alexa 546–conjugated transferrin (Tfn-A546) in cells where pH$_c$ was clamped with

nigericin/K^+. The uptake of Tfn-A546 was largely unaffected at pH 6.8 and much more acidic values had to be reached before a sizable inhibition was detected, in good agreement with earlier data (Sandvig et al., 1987). These findings imply that the inhibition of macropinocytosis seen after a modest acidification was not caused by generalized deleterious effects and provide convenient means for discerning between endocytosis and macropinocytosis.

pH sensitivity of the signals leading to macropinocytosis

Dynamic assessment of the behavior of pH_c-clamped cells by DIC microscopy revealed that the extension of membrane ruffles, rather than their closure to form macropinosomes, was affected by moderate acidification (Video 1). This suggested that an early step in the signaling cascade was impaired by pH. As shown in Fig. 5, phosphorylation of its receptor was robustly stimulated by EGF and this effect persisted in the presence of HOE-694 or in the absence of Na^+. Some inhibition was noted when NHE1 activity was impaired, but this modest (≈30%) decrease was considerably smaller than the effect on TMR-dextran uptake (Fig. 5 B) and therefore unlikely to account for the inhibition of macropinocytosis. This conclusion was supported by experiments where receptor phosphorylation was studied in cells where pH_c was clamped in the absence of Na^+. Under these conditions, only small decreases in phosphorylation were recorded between pH 7.8 and 6.8, whereas macropinocytosis underwent a sharp monotonic decline (Fig. 5 C). Importantly, TMR-dextran uptake declined by >80% between pH 7.4 and 6.8, without discernible change in the extent of receptor phosphorylation. This implies that downstream signaling events must be responsible for most of the pH dependence of macropinocytosis.

Next, we measured the effect of pH_c on the association of the adaptor Grb2 (growth factor receptor-bound protein 2; Liu and Rohrschneider, 2002) with the stimulated receptor by transfecting A431 cells with a fluorescent version of the SH2 domain of Grb2 (Grb2-SH2-YFP). Before stimulation Grb2-SH2-YFP had a cytosolic distribution, but upon EGF addition a fraction redistributed to the plasma membrane, in particular to regions undergoing ruffling (Fig. 6 A). Re-localization of Grb2-SH2-YFP upon EGF stimulation was also observed when Na^+ was replaced by NMG^+, though partial inhibition was noted. More importantly, recruitment of the adaptor to the membrane was essentially identical when pH_c was clamped at pH 7.8 and 6.8 (Fig. 6, A and B). Defective recruitment of Grb2 is therefore unlikely to account for the pH-induced inhibition of macropinocytosis.

The recruitment and activation of PI3K (Cantley, 2002; Hawkins et al., 2006) were studied next. Cells were transfected with a tagged version of the p85β subunit of the kinase and its distribution was assessed by confocal microscopy (Fig. 6, C and D). The regulatory subunit, which was largely cytosolic in unstimulated cells, redistributed to the plasma membrane upon stimulation with EGF. The extent of the recruitment was comparable in cells stimulated in the presence and absence of Na^+ (Fig. 6 D) and was not significantly reduced even when pH_c was

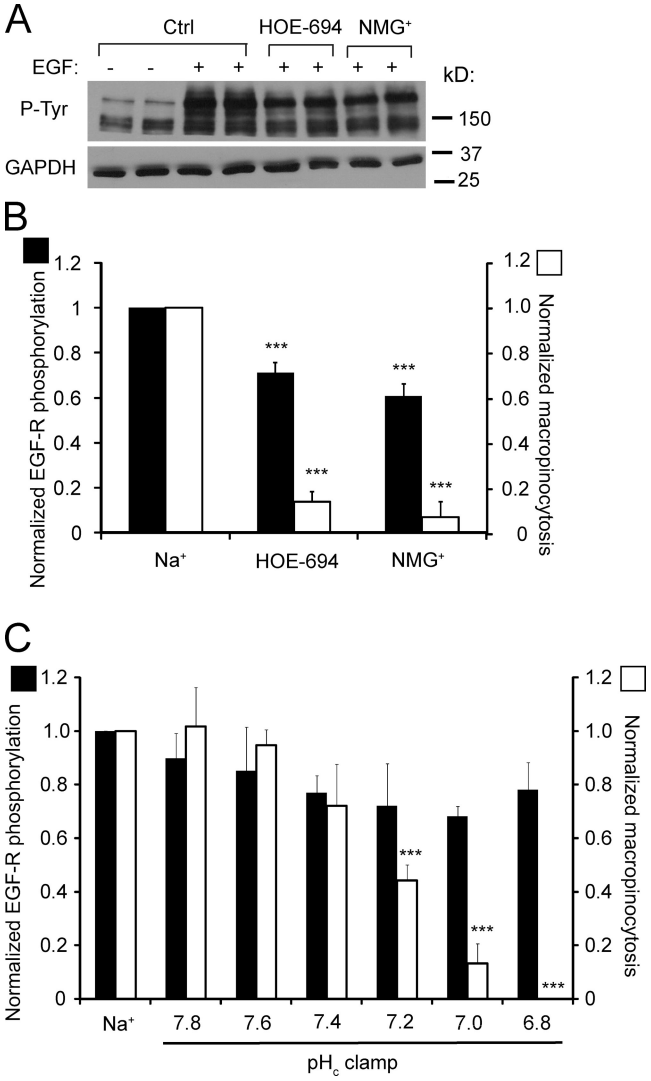

Figure 5. **Effect of NHE inhibition and of cytosolic pH on EGF receptor autophosphorylation.** (A) Immunoblot analysis of tyrosine phosphorylation (P-Tyr) of EGF-R (M_w 170 kD) in A431 cells incubated for 5 min with or without EGF in Na^+-rich buffer, with HOE-694 in Na^+-rich buffer or in NMG^+-rich buffer. Blot is representative of four experiments. (B) Quantitation of the effect of HOE-694 or NMG^+ on EGF-R autophosphorylation, obtained by scanning immunoblots like the one in A (black bars). Data are means ± SE of 4–7 experiments. The effect of the same agents/conditions on macropinocytosis is shown for comparison (open bars). (C) Quantification of EGF-R phosphorylation in cells stimulated in Na^+-rich medium or clamped with nigericin/K^+ at the indicated pH (black bars). Data are means ± SE of 3–4 experiments. Data were normalized to controls in Na^+-rich medium; normalized macropinocytosis is shown for comparison (open bars). ***, $P < 0.001$.

clamped at 6.8. The source of the increased binding noted at pH 7.8 is unclear. Nevertheless, altered localization of the kinase is not the explanation for the impaired macropinocytosis in acidified cells.

The activation of the kinase was assessed next measuring the phosphorylation of Akt, which is recruited to the membrane by phosphatidylinositol-(3,4,5)-trisphosphate (PIP_3), the product of class I PI3K. Akt becomes phosphorylated at the membrane by PDK1 and 2, which are themselves PIP_3-activated kinases (Cantley, 2002; Song et al., 2005). As illustrated in Fig. 6 E, Akt undergoes a marked phosphorylation at Ser473 when cells are stimulated with EGF and this effect is unaltered by HOE-694

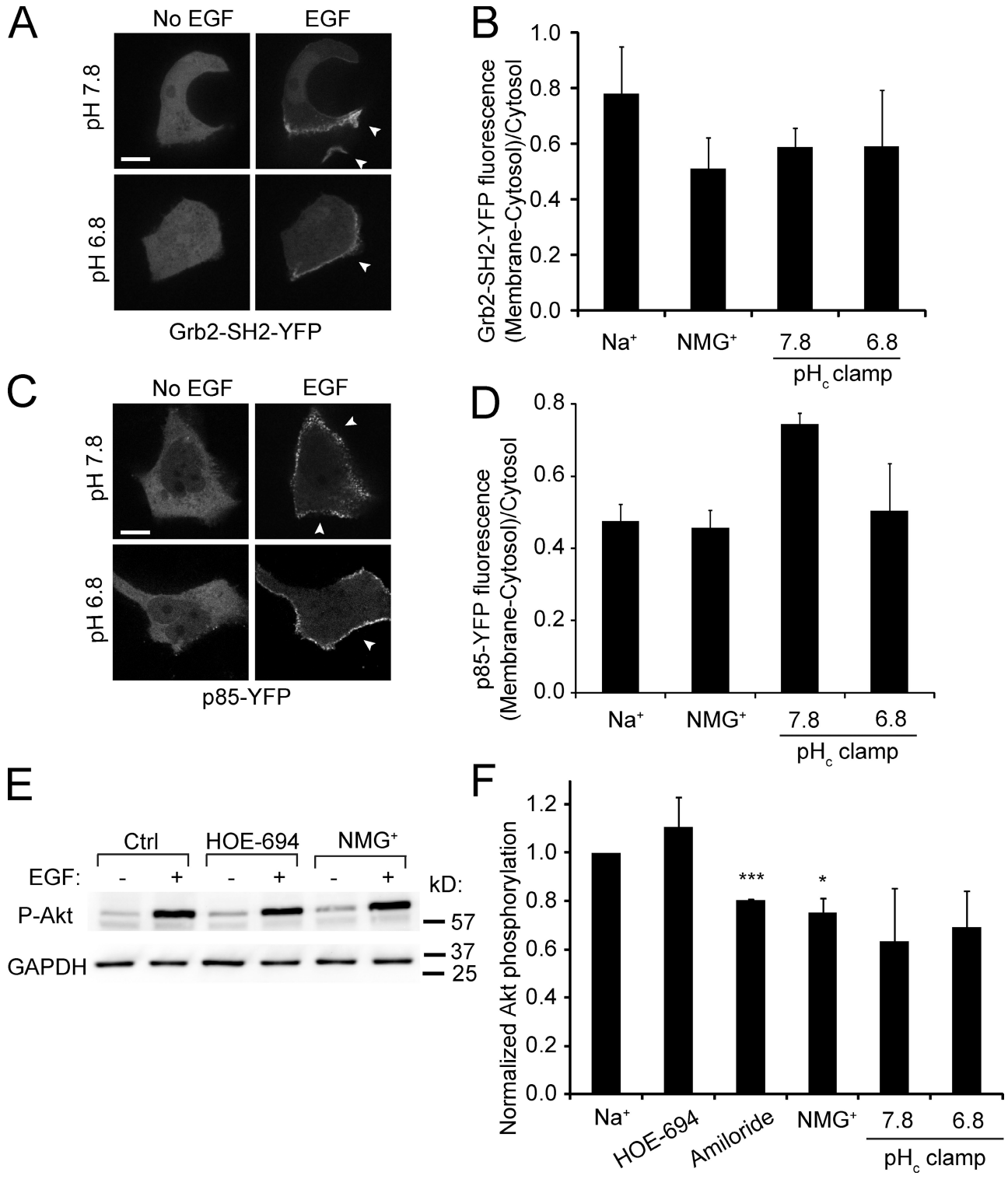

Figure 6. **EGF-induced recruitment of Grb2 and p85β to the membrane and Akt phosphorylation: effect of Na^+ omission and pH.** (A) Confocal images of A431 cells transfected with Grb2-SH2-YFP acquired before and after treatment for 5 min with EGF, while clamping pH_c at the indicated values with nigericin/K^+. (B) Quantification of Grb2-SH2-YFP recruitment to the membrane in response to EGF. Data are means ± SE of 3–4 experiments. (C) Confocal images of cells transfected with p85β-YFP acquired before and after treatment for 5 min with EGF, while clamping pH_c at the indicated values using nigericin/K^+. Arrowheads in A and C point to membrane surface not in contact with neighboring cells. Bar, 10 µm. (D) Quantification of the extent of p85β-YFP recruitment to the membrane in response to EGF. Data are means ± SE of three separate experiments. (E) Immunoblot of Akt Ser473 phosphorylation (P-Akt) in cells incubated for 5 min with EGF in Na^+-rich buffer with or without HOE-694 or in NMG^+-rich buffer. GAPDH was probed in the same blots to ensure comparable loading. Blot is representative of 3–4 similar experiments. (F) Quantification of the effect of NHE inhibitors, Na^+ omission, and pH_c clamping on EGF-induced Akt phosphorylation. Data are means ± SE of ≥3 experiments of each type. *, $P < 0.05$; ***, $P < 0.001$.

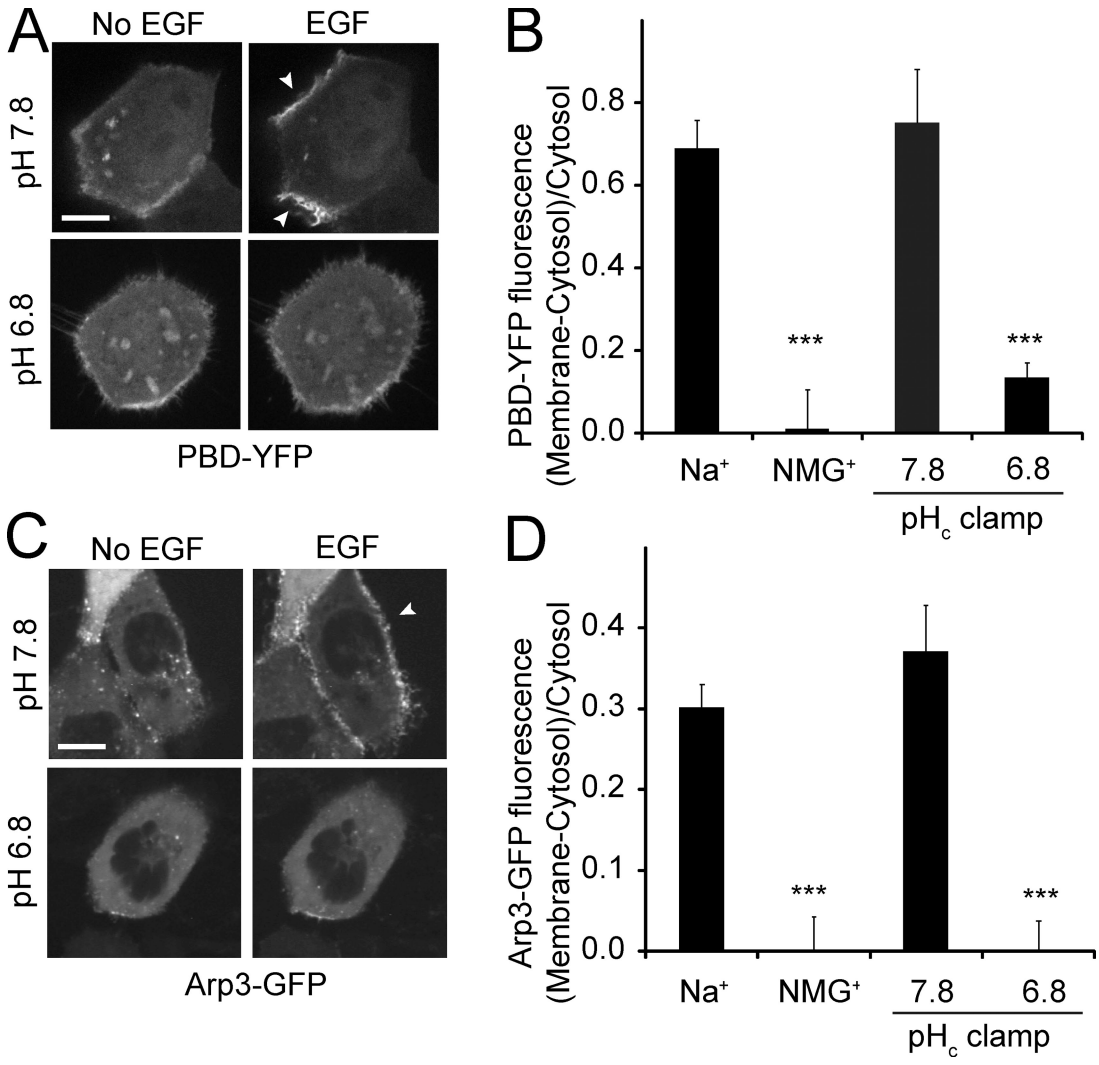

Figure 7. **EGF-induced recruitment of PBD-YFP and Arp3-GFP to the membrane: effect of Na^+ omission and pH.** (A) Confocal images of A431 cells transfected with PBD-YFP acquired before and after treatment for 5 min with EGF, while clamping pH_c at indicated values using nigericin/K^+. Cells with low levels of expression were selected for this experiment. Arrowheads point to membrane surface not in contact with neighboring cells. Bar, 10 µm. (B) Quantification of PBD-YFP recruitment to the membrane in response to EGF. Data are means ± SE of 3–4 separate experiments. (C) Confocal images of cells transfected with Arp3-GFP acquired before and after treatment for 5 min with EGF, while clamping pH_c. (D) Quantification of the extent of Arp3-GFP recruitment to the plasma membrane in response to EGF. Data are means ± SE of 3–4 separate experiments. ***, $P < 0.001$.

or by omission of Na^+. Moreover, a similar degree of phosphorylation was observed when cells were clamped at pH 7.8 and 6.8 (Fig. 6 F). Jointly, these observations indicate that activation of PI3K is not the step responsible for the pH dependence of macropinocytosis.

PIP_3 also serves to target to the membrane and to stimulate guanine nucleotide exchange factors (GEFs) that activate Rho family GTPases (Lemmon et al., 2002; Lindmo and Stenmark, 2006). GEFs like Vav2 and Tiam1 transduce the signals of the PI3K to Rac1 and Cdc42, contributing to membrane ruffling and macropinocytosis (Marcoux and Vuori, 2003; Ridley, 2006; Garrett et al., 2007; Ray et al., 2007). Therefore, we next measured the activation of the GTPases using a fusion protein consisting of the p21-binding domain of PAK fused to YFP (PBD-YFP). This construct binds to the active (GTP-bound) form of Rac1 and to a lesser extent Cdc42 (Srinivasan et al., 2003). In unstimulated cells PBD-YFP was distributed predominantly in the cytosol with little association with the plasma membrane, indicative of a modest tonic activation of Rac1/Cdc42. Upon addition of EGF, however, PBD-YFP accumulated at the ruffling plasma membrane; similar results were obtained in cells bathed in Na^+-rich buffer or pH_c clamped in K^+-rich buffer at 7.8 (Fig. 7, A and B). In sharp contrast, the EGF-induced redistribution of PBD-YFP to the membrane was virtually eliminated when cells were stimulated in Na^+-free, NMG^+-rich buffer. Failure of the construct to relocalize was attributed to the acidification unmasked by omission of Na^+ because similar results were obtained when pH_c was clamped in K^+-rich buffer at 6.8 (Fig. 7, A and B). These results imply that Rac1/Cdc42 activation is impaired by decreased cytosolic pH.

To assess whether decreased pH_c preferentially affects Rac1 or Cdc42, we used two different methods. We initially performed a biochemical assay, sedimenting the active form of the GTPases using immobilized PBD-GST, followed by immunoblotting with

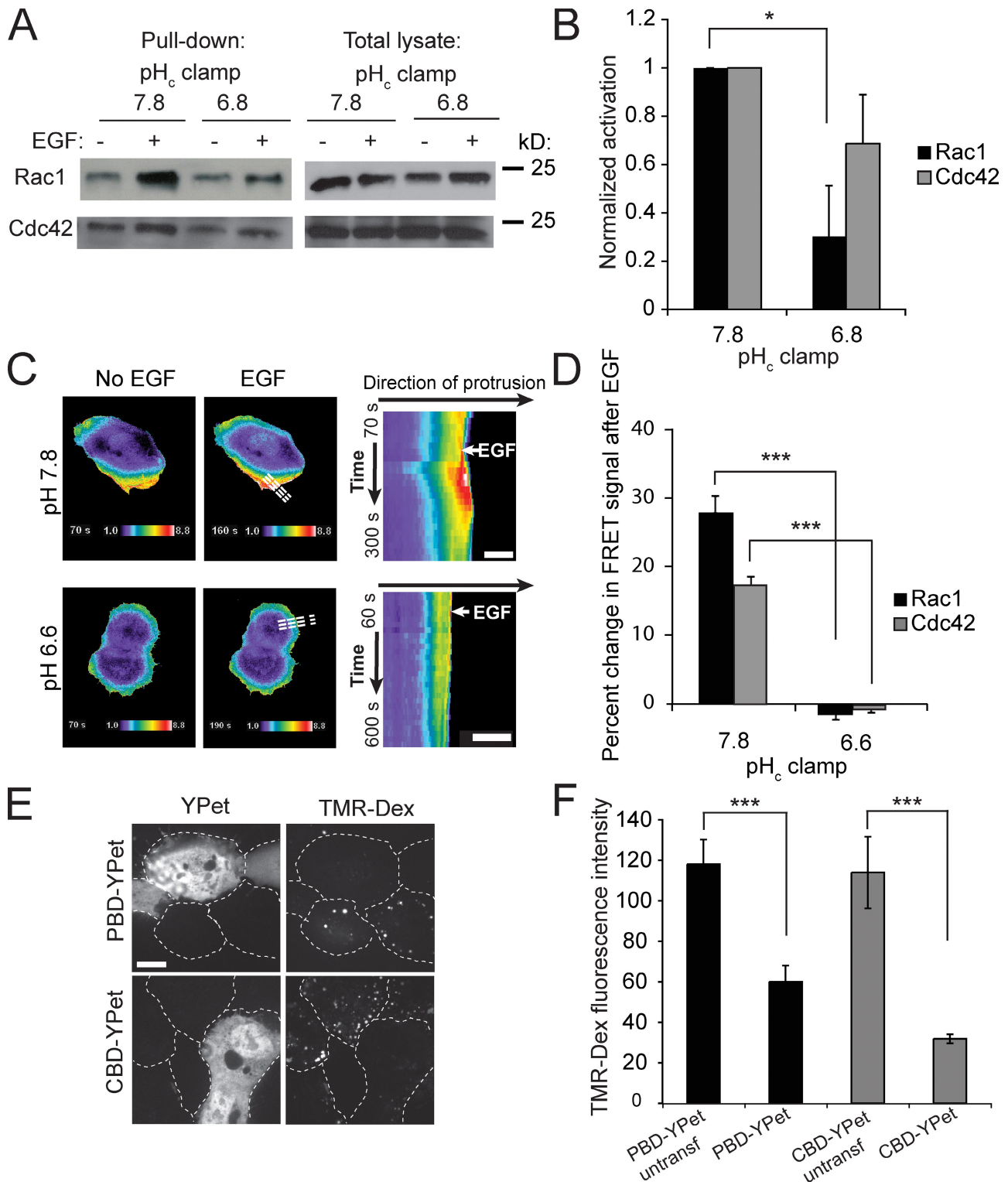

Figure 8. **Effect of pH on activation of Rac1 and Cdc42.** (A) Analysis of activated Rac1 and Cdc42 before and after treatment for 5 min with EGF, while clamping pH_c at the indicated values. Active Rac1 and Cdc42 were pulled down using GST-PBD–coated beads. (B) Quantification of the effect of pH_c-clamping on EGF-induced Rac1 and Cdc42 activation analyzed by GST-PBD pull-down. Data are means ± SE of three experiments. Data were compared between pH_c 7.8 and pH_c 6.8; *, $P < 0.05$. (C) Assessment of Rac1 activation by FRET imaging of genetically encoded biosensors. Activation of Rac1 was measured by FRET as detailed in Materials and methods before and after treatment with EGF, while clamping pH at pH_c 6.6 or pH_c 7.8. Dashed lines in whole-cell images (middle) align with the direction of protrusion and indicate the area selected for kymography and line-scan analysis (right). Bar, 10 µm. (D) Quantification of Rac1 and Cdc42 activation analyzed by FRET using line-scan analysis of the regions studied by kymography as in A. Data are means ± SE of three experiments analyzing 6–8 cells in each; ***, $P < 0.001$. (E) Effect of overexpression or PBD-YPet or CBD-YPet on macropinocytosis. Confocal images of cells transfected with PBD-YPet or CBD-YPet (left) incubated with EGF and TMR-Dextran (right) for 10 min in Na^+-rich medium to assess macropinocytosis. Dashed lines indicate outlines of cells. Bar, 10 µm. (F) Quantification of macropinocytosis in untransfected or in highly transfected cells by measuring TMR-Dextran fluorescence intensity (right). Data are means ± SE of three experiments. Data were compared between untransfected and transfected cells; ***, $P < 0.001$.

Rac1- or Cdc42-specific antibodies. In cells clamped at pH 7.8, both Rac1 and Cdc42 were stimulated by EGF (Fig. 8, A and B), as found earlier (Kurokawa et al., 2004). At pH_c 6.8, however, the activation of both GTPases was depressed. The effect was more apparent for Rac1, which is stimulated more robustly at pH 7.8.

We also analyzed the spatio-temporal dynamics of Rac1 and Cdc42 activation using FRET biosensors (Fig. 8, C and D). A clone of A431 cells that is more amenable to transfection was used for these experiments, which require simultaneous expression of two constructs. This clone also responded to EGF with ruffling and macropinocytosis and the response was largely suppressed at pH 6.6. As shown in Fig. 8 C and Video 2, treatment with EGF induced localized activation of Rac1 at the ruffles and similar, though less robust responses were recorded for Cdc42 (not depicted). When the cytosol was acidified, however, the responses of both GTPases were largely obliterated (Fig. 8, C and D). Thus, the FRET analysis is consistent with the biochemical data, indicating that Rac1 and to a lesser extent Cdc42 are activated by EGF and that both GTPases are sensitive to moderate cytosolic acidification.

The preceding results indicate that Rac1 and Cdc42 are stimulated by EGF, but do not directly link their activity to ruffling and macropinocytosis. A causal relationship was established, taking advantage of the ability of the PBD domain of PAK and the Cdc42/Rac-interacting binding (CRIB) domain of WASP to bind to active Rac1 and Cdc42, respectively. When expressed at low levels, these domains serve as reliable probes of GTPase activation, but when overexpressed they can scavenge away a major fraction of Rac1 or Cdc42 and thereby induce functional inhibition. As shown in Fig. 8, E and F, deliberate overexpression of either PBD-Ypet or CBD-YPet, the PAK-PBD and WASP-CRIB domain constructs, caused inhibition of EGF-induced dextran uptake. Thus, involvement of both Rac1 and Cdc42 is required for optimal macropinocytosis.

Activated Rac1/Cdc42 stimulate WASP and SCAR/WAVE, which induce actin polymerization via the Arp2/3 complex (Ridley, 2006; Swanson, 2008). Based on the preceding results, we anticipated that recruitment of Arp2/3 to the membrane during macropinocytosis would also be highly sensitive to pH_c. This prediction was validated in cells transfected with Arp3-GFP. This indicator was largely cytosolic in unstimulated cells (Fig. 7 C). Addition of EGF prompted a distinct relocalization of Arp3-GFP to the plasma membrane, but this response was only observed in Na^+-rich buffer or when pH_c was clamped at 7.8 using nigericin/K^+. When Na^+ was replaced by NMG^+ or when pH_c was maintained at 6.8, Arp3-GFP remained cytosolic (Fig. 7, C and D). Jointly, these results indicate that activation of the small GTPases Rac1 and Cdc42, and of their downstream effectors that lead to recruitment of Arp2/3 and actin is greatly impaired by a decrease in cytosolic pH, likely accounting for the inhibition of macropinocytosis observed when Na^+/H^+ exchange is blocked.

Role of cofilin

Actin polymerization at sites of membrane protrusion requires elongation of filaments at free barbed ends (FBEs). After activation of small GTPases, actin polymerization is most often mediated by Arp2/3 (Condeelis, 2001) or formins (Goode and Eck, 2007). In addition, FBEs can be generated in stimulated cells by the actin-binding protein cofilin, a process that occurs independently of the Rho family GTPases (Condeelis, 2001; Mouneimne et al., 2004; van Rheenen et al., 2007). Although free cofilin induces severing of actin filaments and generation of FBEs, cofilin is inactive when phosphorylated or when bound to $PI(4,5)P_2$ (Condeelis, 2001; Ridley, 2006). Release from $PI(4,5)P_2$ can occur as a result of hydrolysis of the phosphoinositide, but also because of changes in pH. Frantz et al. (2008) recently demonstrated that cofilin is released from $PI(4,5)P_2$ at alkaline pH, and provided evidence that this contributes to PDGF-induced cell migration. The converse reaction, i.e., the persistent attachment of cofilin to $PI(4,5)P_2$ at more acidic pH, may well explain the inhibitory effect of amiloride on macropinocytosis. We therefore analyzed the role of cofilin in our system.

We studied whether cofilin is activated by dephosphorylation during macropinocytosis. As illustrated in Fig. 9 A, the level of phospho-cofilin in A431 cells in fact increased in response to EGF stimulation, as shown earlier in other cells (Mouneimne et al., 2004; Song et al., 2006). Thus, dephosphorylation does not contribute to cofilin activation in macropinocytosis. Of note, the level of phospho-cofilin was the same in cells clamped at pH_c 7.8 or 6.8, implying that pH had little effect on phosphorylation (unpublished data).

We next considered whether cofilin was released by hydrolysis of $PI(4,5)P_2$, as found in migrating carcinoma cells (Mouneimne et al., 2004; van Rheenen et al., 2007). To this end, we analyzed the fate of the phosphoinositide during macropinocytosis using PLC∂-PH-GFP, a $PI(4,5)P_2$-specific probe. As shown in Fig. 9 B, PLC∂-PH-GFP was present at the membrane before stimulation and, importantly, persisted in the ruffles and even in nascent macropinosomes—identified by trapped rhodamine dextran—disappearing only seconds to minutes after sealing, in accordance with previous data (Araki et al., 2007). Quantification of the density of the probe (Fig. 9 C) confirmed that $PI(4,5)P_2$ did not decrease significantly at the early stages of the process, when actin polymerization is induced. Therefore, release of cofilin as a result of $PI(4,5)P_2$ hydrolysis is unlikely to contribute importantly to actin polymerization.

Even if $PI(4,5)P_2$ remains unaltered, its interaction with cofilin can be weakened by changes in pH (Frantz et al., 2008). We therefore tested whether EGF-induced formation of FBEs, a hallmark of cofilin activation, requires cytosolic alkalinization. As shown in Fig. 9, D and E, the induction of FBEs by EGF could be readily detected in A431 cells. Remarkably, the generation of FBEs persisted when pH was clamped before stimulation at either pH 7.8 or 7.6. Note that elevation of the pH alone, in the absence of EGF, had no discernible effect on FBE formation, implying that alkalinization within the range induced by EGF was insufficient to promote cofilin-induced actin polymerization. Together, these results suggest that an increase in free cytosolic cofilin is not critical to the generation of FBEs or to actin polymerization during macropinocytosis. Accordingly, analysis of the localization of either endogenous or GFP-tagged cofilin indicated that the vast majority of the

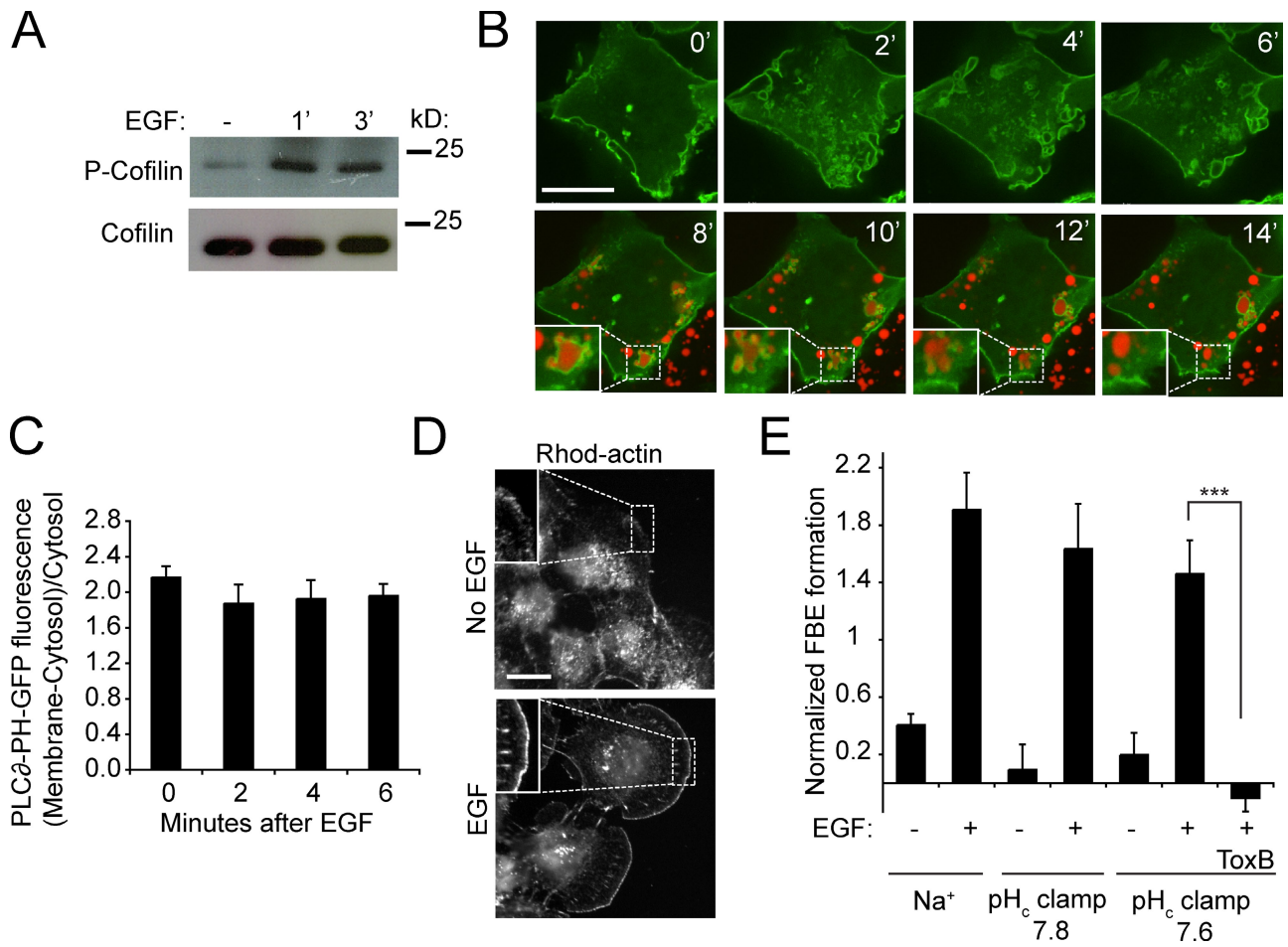

Figure 9. **Cofilin phosphorylation, PI(4,5)P_2 hydrolysis, and actin FBE formation.** (A) Analysis of cofilin phosphorylation from lysates of A431 cells before and after treatment for 1 or 3 min with EGF in Na^+-rich buffer. Blot is representative of three experiments. (B) Assessment of PI(4,5)P_2 hydrolysis during EGF stimulation. PI(4,5)P_2 was monitored using PLC∂-PH-GFP and confocal imaging. Recording was initiated upon addition of EGF and TMR-dextran in Na^+-rich buffer. During the initial 6 min, only green fluorescence was monitored. After 6 min excess TMR-dextran was washed and formed macropinosomes were visualized in red channel. Insets show magnifications of indicated areas. (C) Quantification of PLC∂-PH-GFP localization to the plasma membrane during EGF stimulation. Data are means ± SE of three separate experiments. (D) Detection of actin FBEs by imaging rhodamine-actin in cells before and after treatment for 1 min with EGF in Na^+-rich buffer. Images are representative of three experiments. Insets show regions at the edge of cells typically selected for quantification. (E) Quantification of FBE cells before and after treatment with EGF in Na^+-rich buffer or in pH_c clamping medium. Data are means ± SE of three separate experiments. The significance of the difference ± *C. difficile* toxin B (Tox B) was calculated using Student's *t* test; ***, $P < 0.001$.

protein is cytosolic (Fig. S1) and this distribution was unaltered by EGF stimulation.

Because we failed to implicate cofilin in FBE generation, we tested whether Rho family GTPases were instead involved, possibly through the activation of Arp2/3 and/or formins. Indeed, *C. difficile* toxin B, an inhibitor of Rho GTPases, obliterated the induction of FBEs by EGF (Fig. 9 E).

Discussion

EGF is a potent activator of macropinocytosis. Concomitantly, EGF also stimulates Na^+/H^+ exchange via NHE1. Stimulation of NHE1 by growth promoters, including EGF, has been repeatedly found to induce cytosolic alkalinization, particularly when bicarbonate is omitted (Rothenberg et al., 1983; Ganz et al., 1989; Yanaka et al., 2002). These observations prompted the widely held view that the stimulatory effects of the growth factors were mediated by, or at least required, an increase of pH_c above its resting value. In support of this notion, amiloride and its analogues were reported to preclude the alkalinization and in parallel inhibit cellular proliferation (L'Allemain et al., 1984, 1985; Van Obberghen-Schilling et al., 1985).

Amiloride and HOE-694 also effectively inhibit macropinocytosis (West et al., 1989; Sallusto et al., 1995; Veithen et al., 1996; Meier et al., 2002). Extending the rationale applied to cellular proliferation, it can be postulated that cytosolic alkalosis signals, or is permissive to macropinosome formation. An alternative possibility is that the net osmotic gain associated with Na^+/H^+ exchange drives water influx and swelling of the advancing lamellipodia. Although appealing, these possibilities are not consistent with our data: EGF activated macropinocytosis under conditions where pH_c was maintained at or even slightly below the resting (unstimulated) level. Moreover, macropinocytosis persisted in the absence of Na^+, e.g., when nigericin/K^+ were used to clamp pH_c.

These observations raise the possibility that amiloride analogues may be exerting off-target, nonspecific effects. Indeed,

at high concentrations amiloride directly inhibits autophosphorylation of the EGF receptor (Davis and Czech, 1985). Under the conditions used in our experiments, however, the inhibitory effect of amiloride and its analogues on macropinocytosis appears to be specific, caused by inhibition of NHE1. Indeed, inhibition of exchange by substituting Na^+ for NMG^+ or K^+ (in the absence of nigericin) impaired macropinosome formation (Fig. 3), and HOE-694 had no additional effect when added to Na^+-free solutions. These observations can be reconciled when considering the changes in pH_c induced by EGF. The growth factor stimulates metabolic generation of H^+ equivalents, but these are effectively extruded by NHE1, which is activated concomitantly. Indeed, in the presence of physiological [Na^+] the stimulation of the antiporter outstrips the rate of H^+ generation, resulting in a net alkalinization. The occurrence of a metabolic burst is only unmasked when Na^+/H^+ exchange is prevented (Figs. 2 and 3). We therefore propose that macropinocytosis is not directly sensitive to amiloride or even to inhibition of NHE1, but is instead impaired by the acidification that results when excess H^+ production is uncompensated by the regulatory action of the Na^+/H^+ antiporter.

If macropinocytosis is merely responding to the cytosolic acidification, what makes it uniquely sensitive to amiloride and its analogues? Other endocytic processes, including uptake of transferrin through clathrin-coated pits, are also affected by low pH_c (Davoust et al., 1987; Sandvig et al., 1987; Cosson et al., 1989). However, individual endocytic pathways display differential sensitivity to changes is pH_c: a modest acidification ($pH_c \approx 6.8$) virtually eliminated macropinosome formation, whereas inhibition of clathrin-mediated endocytosis requires a more profound acidification ($pH_c \leq 6.0$; Davoust et al., 1987; Sandvig et al., 1987; Fig. 4). Moreover, geometrical considerations may accentuate the drop in pH experienced during macropinocytosis. When Na^+/H^+ exchange is impaired, the H^+ generated metabolically during signaling and actin polymerization is likely to accumulate in the thin lamellipodia, where diffusional exchange with the bulk cytosolic buffers is restricted. Accordingly, our probes of submembranous pH revealed that during macropinocytosis the acidification is more profound in the immediate vicinity of the receptors than in the cytosol overall. Cell motility, another process dependent on extension of lamellipodia, is similarly sensitive to the pH_c and requires NHE1 for optimal function (Lagana et al., 2000; Denker and Barber, 2002; Stock et al., 2005).

The nature of the pH-sensitive step(s) in macropinocytosis was analyzed by measuring individual events in the signaling cascade while clamping pH_c. Acidification caused only modest changes in receptor phosphorylation (Fig. 5), which in turn had negligible effects on adaptor binding (Fig. 6, A and B) and on recruitment and activation of PI3K (Fig. 6, C–F), a key reaction in macropinosome formation. In contrast, the activation of Rac1/Cdc42 and their effectors was profoundly inhibited (Figs. 7 and 8). This conclusion is consistent with earlier observations of Frantz et al. (2007), who noted the pH dependence of Cdc42 activation at the leading edge of migrating cells. We therefore conclude that the exchange factors that activate Rac1/Cdc42 and/or the GTPases themselves are highly sensitive to pH_c. Tiam1, Vav2, and Dock180 have been implicated in epidermal growth factor receptor (EGFR)–mediated activation of Rac1 and Cdc42 (Marcoux and Vuori, 2003; Tamás et al., 2003; Makino et al., 2006; Ray et al., 2007). We attempted to determine the effect of pH on these GEFs, but failed to observe consistent recruitment of either Vav2 or Dock180 to the membrane of EGF-stimulated A431 cells. Tiam1, instead, was constitutively associated with the membrane, as reported previously (Michiels et al., 1995). We did not notice any significant changes in its distribution when pH_c was lowered from 7.8 to 6.8, and are therefore unable to attribute the effects of pH to this GEF. We also considered the possibility that acidification might affect the targeting or retention of the GTPases in the membrane by altering the surface charge. A polycationic stretch near the farnesylated C terminus of Rac1 and Cdc42 is thought to contribute to their targeting to the negatively charged plasmalemma (Heo et al., 2006). To this end, cells were transfected with the constitutively active Rac1-Q61L-GFP or with the charge-sensitive probe R-Pre-mRFP, and their localization was visualized at pH_c 7.8 and 6.8 (Fig. S2). Lowering pH_c to 6.8, however, had no effect on the localization of these probes, suggesting that altered membrane charge is not the likely explanation for the reduced activation of the GTPases.

Other downstream steps or parallel pathways are also likely to be impaired by cytosolic acidification during macropinocytosis. One such target of pH_c is cofilin, an actin-severing protein that generates new FBEs (Condeelis, 2001; van Rheenen et al., 2007). Frantz et al. (2008) showed that cofilin binding to $PI(4,5)P_2$ is pH sensitive, the affinity of the interaction weakening as the cytosol becomes alkaline. The NHE-mediated alkalosis induced by growth factors would be expected to release cofilin, contributing to FBE formation and actin polymerization. The converse reaction, i.e., the persistent attachment of cofilin to $PI(4,5)P_2$ at more acidic pH, could explain the inhibitory effect of amiloride on macropinocytosis. Our experimental evidence, however, argues against this mechanism and against a major role of cofilin in EGF-induced actin polymerization in A431 cells. First, cofilin phosphorylation, which is predicted to inactivate the protein, increased upon EGF stimulation. Second, we found no evidence for cofilin release from the membrane as a result of $PI(4,5)P_2$ hydrolysis. Third, and most important, we failed to detect any effect of the pH-dependent release of cofilin from $PI(4,5)P_2$ on FBE formation or actin polymerization. Mimicking the alkalinization induced by EGF was insufficient to induce FBE or discernible F-actin formation, whereas stimulation with the growth factor under conditions where pH remained clamped at prestimulation levels markedly activated FBE formation and actin polymerization (Fig. 9). Moreover, the polymerization of actin and accompanying ruffling precede the alkalinization induced by EGF (Fig. 2 A). Therefore, the sensitivity of cofilin to pH cannot explain the effects of amiloride on macropinocytosis.

Irrespective of the exact mechanism whereby decreased cytosolic pH affects small GTPase activation and actin assembly, our results indicate that amiloride and related compounds are neither direct nor specific inhibitors of macropinocytosis. Their inhibitory effects are the consequence of submembranous

acidification caused by metabolic H^+ generation, unopposed by the regulatory extrusion across the membrane. The unique sensitivity of macropinocytosis, compared with other endocytic processes, results from a complex convergence of circumstances: a large and sustained metabolic burst that occurs within a diffusionally constrained compartment, the thin lamellipod. These considerations must be taken into account when using amiloride analogues as hallmarks of macropinocytosis because not only are other processes likely to be inhibited by the pH change, but macropinocytosis can overcome the inhibitory effects of these compounds if means other than NHE1 are provided to regulate pH_c.

Materials and methods

Materials

The acetoxymethyl-ester of SNARF-5, nigericin, EGF, TMR-dextran (M_w 10,000), transferrin-Alexa 546, and rhodamine-phalloidin were from Invitrogen. HOE-694 was a gift from Dr. H.-J. Lang (Aventis Pharma, Frankfurt am Main, Germany). Lipofectamine LTX was from Invitrogen, Fugene6 from Roche, LY294002 from Enzo Life Sciences, Inc., latrunculin B from EMD, G-Sepharose beads from GE Healthcare, and rabbit skeletal muscle rhodamine-actin from Cytoskeleton, Inc. Mouse monoclonal anti-phosphotyrosine (4G10) and anti-GAPDH antibodies were from Millipore, rabbit monoclonal anti-phospho-Akt (Ser 473) antibody was from Cell Signaling Technology, mouse monoclonal anti-Rac1 and anti-Cdc42 were from BD, and rabbit polyclonal anti-cofilin and anti–phospho-cofilin were from Abcam. All other chemicals were from Sigma-Aldrich.

Isotonic Na^+-rich buffer contained 140 mM NaCl, 3 mM KCl, 1 mM $MgCl_2$, 1 mM $CaCl_2$, 5 mM glucose ,and 20 mM Hepes, pH 7.4. In NMG^+-rich buffer NaCl and KCl were replaced by 143 mM NMG-chloride, and in K^+-rich buffer NaCl was replaced by 100 mM K-glutamate and 43 mM KCl.

Cell culture and constructs

A431 cells were from American Type Culture Collection (Rockville, MD) and were grown in DMEM with 10% fetal bovine serum at 37°C under 5% CO_2. Before experiments the cells were serum starved for 2–16 h. PBD-YFP was a gift from Dr. G. Bokoch (The Scripps Research Institute, La Jolla, CA). Mouse p85β-YFP was plasmid #1408 from Addgene, deposited by Dr. L. Cantley (Harvard Medical School, Boston, MA). R-Pre-mRFP and Rac1Q61L-GFP (Yeung et al., 2006) as well as PLCδ-PH-GFP (Várnai and Balla, 2008) have been described previously. Membrane-targeted SuperEcliptic (SE) pHluorin/mCherry was generated by first constructing a chimeric construct consisting of the green, pH-sensitive fluorescent protein SEpHluorin (a gift of Dr. J. Rothman, Columbia University, New York, NY; Miesenböck et al., 1998; Sankaranarayanan et al., 2000) fused to the red, pH-insensitive mCherry (Shu et al., 2006). The EGFP coding region from the EGFP-N1 vector (Takara Bio, Inc.) was replaced with a PCR product containing the SEpHluorin coding region flanked by BamHI and NotI restriction sites. The PCR product of the mCherry coding sequence was inserted at the EcoRI and BamHI sites. The probe was targeted to the plasma membrane by inclusion of the N-terminal motif of the Src family kinase Lyn (Corbett-Nelson et al., 2006). The membrane targeting sequence of Lyn was inserted between XhoI and EcoRI sites. The forward and reverse oligonucleotide sequences for the Lyn membrane targeting sequence were 5′-tcgagagaaatatgggatgtattaaatcaaaaaggaaagacgggAg-3′ and 5′-aattctcccgtctttccttttgatttaatacatcccatatttctc-3′, respectively.

The Rac1 FRET biosensor was reported previously (Kraynov et al., 2000; Machacek et al., 2009), and here includes modifications to improve FRET efficiency reported in Machacek et al. (2009). The Cdc42 biosensor uses an intermolecular design as reported by several groups (Itoh et al., 2002; Seth et al., 2003; Tzima et al., 2003; Hoppe and Swanson, 2004), but here is further optimized by the use of different fluorescent proteins and of a Cdc42-binding domain from WASP, a fragment shown to provide good selectivity for activated Cdc42 in a previously developed biosensor with a different design (Nalbant et al., 2004; Frantz et al., 2007; Machacek et al., 2009). Both biosensors were generated by first constructing plasmids encoding either Rac1 or Cdc42 fused to the C terminus of CyPet, a CFP variant optimized for FRET (Nguyen and Daugherty, 2005), and either the CRIB domain from p21-activated kinase (PBD) published previously (Machacek et al., 2009) or the Cdc42-binding CRIB domain from WASP (CBD), amino acids 230–314, fused to the C terminus of YPet, a YFP variant optimized for FRET (Nguyen and Daugherty, 2005). The EGFP coding region from the EGFP-C1 vector (Takara Bio, Inc.) was replaced with a PCR product containing the CyPet or YPet coding regions flanked by an NcoI restriction site and a SGLASELGS linker containing a BamHI restriction site. The PCR products of the Rac1, Cdc42, PBD, and CBD coding sequences were inserted between the BamHI restriction site in the SGLASELGS linker and an EcoRI restriction site in the downstream multiple cloning site of the vector.

The plasmids were transfected into A431 cells using Lipofectamine LTX, Fugene6, or the Amaxa Nucleofection kit according to the manufacturer's instructions.

pH measurements

The effect of HOE-694 on NHE1 activity was measured as the rate of Na^+-induced recovery of pH_c after an acid load. Dual-emission ratio fluorescence (640/590 nm) of SNARF-5F was used to measure pH_c at 37°C. Serum-starved cells grown on 18-mm coverslips were placed into Chamlid imaging chambers (Live Cell Instrument, Inc.), loaded with 20 µM SNARF-5F acetoxymethyl-ester for 20 min at 37°C and prepulsed with 30 mM NH_4Cl in Na^+-rich buffer for 10 min. Cells were acidified by NH_4Cl removal with NMG^+-rich buffer, and Na^+/H^+ exchange initiated by reintroduction of Na^+-rich buffer with or without HOE-694. pH_c was calibrated using K^+-rich buffer containing 10 µg/ml nigericin (pH_c-clamping buffer) as described previously (Thomas et al., 1979). pH_{sm} was assessed by transfecting the cells with membrane-targeted SEpHluorin/mCherry, measuring the SEpHluorin/mCherry fluorescence emission ratio at the plasma membrane by spinning disc confocal microscopy using conventional optics for green and red fluorophores, and calibrating with K^+/nigericin as above. pH_c measured by soluble SEpHluorin was assessed similarly, but the fluorescence was captured by epifluorescence as detailed below.

Macropinocytosis and endocytosis assays

To measure macropinocytosis, serum-starved A431 cells grown on coverslips and placed in Chamlid chambers were incubated with 0.5 mg/ml TMR-dextran and, where noted, stimulated with 100–200 ng/ml EGF in the indicated buffer for 10 min at 37°C. Cells were washed and both DIC and red fluorescence images of live cells were acquired. Where indicated, the following inhibitors were used: 10 µM latrunculin B, 100 µM LY294002, 1 mM amiloride, or 10 µM HOE-694. In the case of latrunculin B and LY294002 the cells were preincubated with the inhibitors at 37°C for 30 min before EGF addition. Macropinocytosis was quantified as the number of cells containing macropinosomes in the cells outlining each island.

Endocytosis was assessed by incubating the cells with 50 µg/ml Alexa 546–conjugated transferrin in the indicated buffer for 15 min at 37°C, after which the cells were placed on ice and acid washed with 0.2 M acetic acid in 150 mM NaCl and PBS to remove exofacial fluorescence. The cells were then fixed and mounted on slides, and red fluorescence was imaged and quantified.

Functional assays in pH_c-clamped cells

To clamp pH_c, the cells were preincubated at 37°C for 5 min in the presence of 10 µg/ml of the K^+/H^+ ionophore nigericin in K^+-rich buffer (K^+/nigericin) of predetermined pH before the addition of 100–200 ng/ml EGF.

Fluorescence microscopy

Imaging of live cells was performed at 37°C in isotonic Na^+-rich buffer or in isotonic K^+- or NMG^+-rich buffer or pH_c-clamping buffer as indicated. pH_c measurements were performed using a microscope (model DM IRB; Leica) equipped with filter wheels (Sutter Instruments) to independently alternate between 640- and 590-nm emissions for SNARF5-F (Steinberg and Grinstein, 2007) or using conventional optics for green and red for soluble SEpHluorin/mCherry. Light from an EXFO X-Cite 120 lamp (Exfo Life Sciences Group) was directed to the sample by using a dichroic mirror. A Plan-Apo 40x/NA 1.25 oil immersion objective was used. Emitted light was captured by a CCD camera (Cascade II; Photometrics). The filter wheel and camera were under the control of MetaMorph/MetaFluor software (MDS Analytical Technologies). pHc measured with soluble SEpHluorin was performed with the same system as above. The fluorescence of TMR-dextran taken up by macropinocytosis, transferrin–Alexa 546 taken up by endocytosis, rhodamine-phalloidin as well as rhodamine-actin were imaged with a microscope (model DMIRE2; Leica) using a 63x or 100x/NA 1.4 oil immersion objective under the illumination of an

EBQ100 lamp and using conventional optics for red fluorophores. Images were captured by a CCD camera (model C4742-95-12ER; Hamamatsu Photonics) under the control of Openlab software (PerkinElmer).

Imaging of transfected cells for construct localization analysis as well as pH_{sm} measurements were performed on a spinning disc confocal microscopy system (Quorum Technologies, Inc.) based on an Axiovert 200M microscope (Carl Zeiss, Inc.), as detailed previously (Yeung et al., 2008). Cells were maintained at 37°C using an environmental control system (Live Cell Instrument). The samples were excited with diode-pumped solid-state laser lines (Applied Research) using a 491-nm laser line and 520-nm emission filter for GFP, YFP, and SEpHluorin, and a 561-nm laser line and 590-nm emission filter for mCherry and mRFP. A 63x/NA 1.4 oil immersion objective was used. Images were acquired using a back-thinned electron multiplier CCD camera (C9100-13 ImagEM; Hamamatsu Photonics) driven by Volocity 4.1.1 software (PerkinElmer).

The software used for subsequent image analysis was MetaFluor for pH_c measurements and Volocity 4.1.1 for construct localization analysis and all the other fluorescence intensity quantifications. All the quantifications were performed on background-subtracted images with 3–10 cells analyzed in each experiment.

Rac1 and Cdc42 activity assays

The abundance of active (i.e., GTP-bound) small GTPases was quantified by immunoblotting after a GST-PAK-PBD pull-down step, as described previously (Di Ciano et al., 2002).

Activation of both Rac1 and Cdc42 by FRET was measured in living cells by monitoring the ratio of FRET (CyPet excitation and YPet emission channels) to CyPet emission (CyPet excitation and emission channels), correcting for emission bleed-through as described previously (Hodgson et al., 2009) and briefly below. Cells were chosen for low expression levels so that neither PBD-YPet nor CBD-YPet inhibited macropinocytosis. Time-lapse sequences were acquired on an inverted epifluorescence microscope (model IX81; Olympus), using a 40X UPlan FLN 1.3 N/A DIC lens (Olympus), CCD camera (CoolSnapESII; Roper Industries), and MetaMorph software. For emission ratio imaging, the following filter sets were used (Chroma Technology Corp.): CyPet: D436/20, D470/40; FRET: D436/20, HQ535/30; YPet: HQ500/20, HQ535/30. A dichroic mirror was custom manufactured by Chroma Technology Corp. for compatibility with all of these filters. Cells were illuminated with a 100-W Hg lamp through an ND 1.0 neutral density filter. At each time point, three images were recorded with the following exposure times: CyPet (1.2 s), FRET (1.2 s), and YPet (0.4 s) with 2 × 2 binning. We routinely changed the order of acquisition for all experiments to control for motion artifacts, using either the order CyPet, FRET, YPet; or FRET, CyPet, YPet. We have used this approach previously to show that the order of data acquisition did not affect the measured ratio (Nalbant et al., 2004; Pertz et al., 2006). In addition, measurements of cells obtained in forward and reverse order were combined in the final analysis. Time-lapse sequences were recorded at 10- or 20-s intervals between frames for all biosensors, as described previously (Pertz et al., 2006; Hodgson et al., 2009).

Ratio calculations to generate activity images were performed after bleed-through and photobleaching correction methods described previously (Hodgson et al., 2009) because each component of the two chain biosensor is not necessarily distributed equally throughout the cell. For bleed-through correction, cells expressing CyPet or YPet alone were imaged using the same imaging medium, exposure times, and intensities as those listed above for the actual experiment. These measurements were used to determine the amount of bleed-through of each fluorescent protein's direct emission into the FRET channel. Images from each channel were shade corrected and background subtracted. Plotting FRET intensity as the dependent variable versus CyPet or YPet intensity as the independent variable yielded a linear relationship where the slope of the line defined the bleed-through coefficient for that fluorescent protein and condition (0.25 for CyPet and 0.15 for YPet using the conditions above). Using these parameters, the ratio was derived using Eq. 1:

$$\text{FRET Ratio} = \frac{\text{FRET} - \alpha \cdot \text{CyPet} - \beta \cdot \text{YPet}}{\text{CyPet}} \quad (1)$$

This equation corrects the raw FRET signal for bleedthrough from both CyPet and YPet into the FRET channel, with subsequent calculation of the ratio.

For visual representations, a linear pseudocolor look-up table was applied to all ratio images and the ratio values were normalized to the lower scale value, which was chosen to exclude the bottom 5% of the total histogram distribution, thereby avoiding spurious low intensity pixels. In each experiment, all images were carefully inspected to verify that all portions used to create the ratio image had a sufficiently high signal-to-noise ratio. We targeted at least 300 gray level values (12-bit dynamic range) above background in the lowest intensity regions within the cell ($S/n > 3$). This was especially important in thin parts of the cell where fluorescence was low.

Actin-free barbed end assay

Actin-free barbed ends were determined by a modification of previously described methods (Chan et al., 1998; Frantz et al., 2008). In short, serum-starved A431 cells on coverslips were incubated with or without EGF in Na^+-rich or pH_c-clamping buffer for 1 or 3 min. To inhibit Rho GTPases, cells were incubated in the presence of *C. difficile* toxin B (50 ng/ml) for 3 h before EGF stimulation. To label FBEs the cells were permeabilized for 15 s in a buffer (20 mM Hepes, 140 mM NaCl, 3 mM KCl, 2 mM $MgCl_2$, 2 mM EGTA, 5 mM glucose, 1% BSA, and 0.5 mM ATP, pH 7.5) containing 0.04% saponin and 0.02 µg/µl rhodamine-labeled rabbit skeletal muscle actin. After 15 s the solution was diluted with a 3x volume of permeabilization buffer without saponin and rhodamine-actin, and incubation continued for 3 min followed by fixation. The extent of FBE formation was calculated by measuring fluorescence intensity of a band 0.3–0.5 µm wide at the edge of the cell (the edge of the protruding lamellipod in stimulated cells) and a band of the same width (~0.5 µm) inside the cell. The fluorescence intensity is reported as the ratio of the fluorescence at the edge to that in the cytosol, and comparison between experiments was facilitated by normalizing to the cytosolic fluorescence.

Other methods

Samples for Western blotting were scraped off the substratum in the presence of protease inhibitors (Sigma-Aldrich), 1 mM PMSF, 1 mM Na_3VO_4, and 0.1 µM okadaic acid, subjected to SDS-PAGE, and transferred to nitrocellulose filters which were then blocked with 5% BSA or milk in TBS-Tween. The primary antibody dilutions used were 1:10,000 for anti-P-Tyr, 1:5,000 for anti-P-Akt, 1:10,000 for anti-GAPDH, 1:1,000 for anti-Rac1 and Cdc42, 1:1,000 for anti–phospho-cofilin, and 1:10,000 for anti-cofilin. After incubating with horseradish peroxidase–conjugated secondary antibody the chemiluminescence of the immunoreactive bands was quantified using the Fluorchem FC2 chemiluminescence system (Alpha Innotech). To visualize actin, cells were fixed with 4% paraformaldehyde, permeabilized, and stained with rhodamine-phalloidin.

Online supplemental material

Fig. S1 shows cofilin localization during macropinocytosis. Fig. S2 shows the effect of cytosolic pH on the localization of surface charge probes. Video 1 is a DIC illustration of the effect of pH_c clamping on membrane protrusions during EGF stimulation. Video 2 depicts Rac1 FRET ratio in pH_c-clamped, EGF-stimulated cells. Online supplemental material is available at http://www.jcb.org/cgi/content/full/jcb.200908086/DC1.

We thank Dr. Caterina DiCiano-Oliveira for help with PBD pull-downs and Dr. Michael Glogauer for help with the FBE assay.

This work was supported by grant MOP4665 of the Canadian Institutes of Health Research and a grant from the Ella and Georg Ehrnrooth Foundation to M. Koivusalo. We gratefully acknowledge funding from National Institutes of Health grants GM57464 and GM64346 (to K.M. Hahn), T32 GM008719, and F30 F30HL094020-02 (to C. Welch). S. Grinstein holds the Pitblado Chair in Cell Biology and is cross-appointed to the Department of Biochemistry of the University of Toronto.

Submitted: 17 August 2009
Accepted: 25 January 2010

References

Alvarez de la Rosa, D., C.M. Canessa, G.K. Fyfe, and P. Zhang. 2000. Structure and regulation of amiloride-sensitive sodium channels. *Annu. Rev. Physiol.* 62:573–594. doi:10.1146/annurev.physiol.62.1.573

Amyere, M., B. Payrastre, U. Krause, P. Van Der Smissen, A. Veithen, and P.J. Courtoy. 2000. Constitutive macropinocytosis in oncogene-transformed fibroblasts depends on sequential permanent activation of phosphoinositide 3-kinase and phospholipase C. *Mol. Biol. Cell.* 11:3453–3467.

Amyere, M., M. Mettlen, P. Van Der Smissen, A. Platek, B. Payrastre, A. Veithen, and P.J. Courtoy. 2002. Origin, originality, functions, subversions and molecular signalling of macropinocytosis. *Int. J. Med. Microbiol.* 291:487–494. doi:10.1078/1438-4221-00157

Araki, N., M.T. Johnson, and J.A. Swanson. 1996. A role for phosphoinositide 3-kinase in the completion of macropinocytosis and phagocytosis by macrophages. *J. Cell Biol.* 135:1249–1260. doi:10.1083/jcb.135.5.1249

Araki, N., Y. Egami, Y. Watanabe, and T. Hatae. 2007. Phosphoinositide metabolism during membrane ruffling and macropinosome formation in EGF-stimulated A431 cells. *Exp. Cell Res.* 313:1496–1507. doi:10.1016/j.yexcr.2007.02.012

Cantley, L.C. 2002. The phosphoinositide 3-kinase pathway. *Science.* 296:1655–1657. doi:10.1126/science.296.5573.1655

Cardelli, J. 2001. Phagocytosis and macropinocytosis in *Dictyostelium*: phosphoinositide-based processes, biochemically distinct. *Traffic.* 2:311–320. doi:10.1034/j.1600-0854.2001.002005311.x

Chan, A.Y., S. Raft, M. Bailly, J.B. Wyckoff, J.E. Segall, and J.S. Condeelis. 1998. EGF stimulates an increase in actin nucleation and filament number at the leading edge of the lamellipod in mammary adenocarcinoma cells. *J. Cell Sci.* 111:199–211.

Condeelis, J. 2001. How is actin polymerization nucleated in vivo? *Trends Cell Biol.* 11:288–293. doi:10.1016/S0962-8924(01)02008-6

Corbett-Nelson, E.F., D. Mason, J.G. Marshall, Y. Collette, and S. Grinstein. 2006. Signaling-dependent immobilization of acylated proteins in the inner monolayer of the plasma membrane. *J. Cell Biol.* 174:255–265. doi:10.1083/jcb.200605044

Cosson, P., I. de Curtis, J. Pouysségur, G. Griffiths, and J. Davoust. 1989. Low cytoplasmic pH inhibits endocytosis and transport from the trans-Golgi network to the cell surface. *J. Cell Biol.* 108:377–387. doi:10.1083/jcb.108.2.377

Counillon, L., W. Scholz, H.J. Lang, and J. Pouysségur. 1993. Pharmacological characterization of stably transfected Na+/H+ antiporter isoforms using amiloride analogs and a new inhibitor exhibiting anti-ischemic properties. *Mol. Pharmacol.* 44:1041–1045.

Davis, R.J., and M.P. Czech. 1985. Amiloride directly inhibits growth factor receptor tyrosine kinase activity. *J. Biol. Chem.* 260:2543–2551.

Davoust, J., J. Gruenberg, and K.E. Howell. 1987. Two threshold values of low pH block endocytosis at different stages. *EMBO J.* 6:3601–3609.

Denker, S.P., and D.L. Barber. 2002. Cell migration requires both ion translocation and cytoskeletal anchoring by the Na-H exchanger NHE1. *J. Cell Biol.* 159:1087–1096. doi:10.1083/jcb.200208050

Dharmawardhane, S., A. Schürmann, M.A. Sells, J. Chernoff, S.L. Schmid, and G.M. Bokoch. 2000. Regulation of macropinocytosis by p21-activated kinase-1. *Mol. Biol. Cell.* 11:3341–3352.

Di Ciano, C., Z. Nie, K. Szászi, A. Lewis, T. Uruno, X. Zhan, O.D. Rotstein, A. Mak, and A. Kapus. 2002. Osmotic stress-induced remodeling of the cortical cytoskeleton. *Am. J. Physiol. Cell Physiol.* 283:C850–C865.

Falcone, S., E. Cocucci, P. Podini, T. Kirchhausen, E. Clementi, and J. Meldolesi. 2006. Macropinocytosis: regulated coordination of endocytic and exocytic membrane traffic events. *J. Cell Sci.* 119:4758–4769. doi:10.1242/jcs.03238

Frantz, C., A. Karydis, P. Nalbant, K.M. Hahn, and D.L. Barber. 2007. Positive feedback between Cdc42 activity and H+ efflux by the Na-H exchanger NHE1 for polarity of migrating cells. *J. Cell Biol.* 179:403–410. doi:10.1083/jcb.200704169

Frantz, C., G. Barreiro, L. Dominguez, X. Chen, R. Eddy, J. Condeelis, M.J. Kelly, M.P. Jacobson, and D.L. Barber. 2008. Cofilin is a pH sensor for actin free barbed end formation: role of phosphoinositide binding. *J. Cell Biol.* 183:865–879. doi:10.1083/jcb.200804161

Ganz, M.B., G. Boyarsky, R.B. Sterzel, and W.F. Boron. 1989. Arginine vasopressin enhances pHi regulation in the presence of HCO_3^- by stimulating three acid-base transport systems. *Nature.* 337:648–651. doi:10.1038/337648a0

Garrett, W.S., L.M. Chen, R. Kroschewski, M. Ebersold, S. Turley, S. Trombetta, J.E. Galán, and I. Mellman. 2000. Developmental control of endocytosis in dendritic cells by Cdc42. *Cell.* 102:325–334. doi:10.1016/S0092-8674(00)00038-6

Garrett, T.A., J.D. Van Buul, and K. Burridge. 2007. VEGF-induced Rac1 activation in endothelial cells is regulated by the guanine nucleotide exchange factor Vav2. *Exp. Cell Res.* 313:3285–3297. doi:10.1016/j.yexcr.2007.05.027

Goode, B.L., and M.J. Eck. 2007. Mechanism and function of formins in the control of actin assembly. *Annu. Rev. Biochem.* 76:593–627. doi:10.1146/annurev.biochem.75.103004.142647

Grinstein, S., S. Cohen, J.D. Goetz, A. Rothstein, and E.W. Gelfand. 1985. Characterization of the activation of Na+/H+ exchange in lymphocytes by phorbol esters: change in cytoplasmic pH dependence of the antiport. *Proc. Natl. Acad. Sci. USA.* 82:1429–1433. doi:10.1073/pnas.82.5.1429

Grinstein, S., D. Rotin, and M.J. Mason. 1989. Na+/H+ exchange and growth factor-induced cytosolic pH changes. Role in cellular proliferation. *Biochim. Biophys. Acta.* 988:73–97.

Hawkins, P.T., K.E. Anderson, K. Davidson, and L.R. Stephens. 2006. Signalling through Class I PI3Ks in mammalian cells. *Biochem. Soc. Trans.* 34:647–662. doi:10.1042/BST0340647

Heo, J., K.W. Raines, V. Mocanu, and S.L. Campbell. 2006. Redox regulation of RhoA. *Biochemistry.* 45:14481–14489. doi:10.1021/bi0610101

Hodgson, L., F. Shen, and K. Hahn. 2009. Biosensors for characterizing the dynamics of Rho family GTPases in living cells. *Curr. Protoc. Cell Biol.* In press.

Hoppe, A.D., and J.A. Swanson. 2004. Cdc42, Rac1, and Rac2 display distinct patterns of activation during phagocytosis. *Mol. Biol. Cell.* 15:3509–3519. doi:10.1091/mbc.E03-11-0847

Itoh, R.E., K. Kurokawa, Y. Ohba, H. Yoshizaki, N. Mochizuki, and M. Matsuda. 2002. Activation of rac and cdc42 video imaged by fluorescent resonance energy transfer-based single-molecule probes in the membrane of living cells. *Mol. Cell. Biol.* 22:6582–6591. doi:10.1128/MCB.22.18.6582-6591.2002

Kraynov, V.S., C. Chamberlain, G.M. Bokoch, M.A. Schwartz, S. Slabaugh, and K.M. Hahn. 2000. Localized Rac activation dynamics visualized in living cells. *Science.* 290:333–337. doi:10.1126/science.290.5490.333

Kurokawa, K., R.E. Itoh, H. Yoshizaki, Y.O. Nakamura, and M. Matsuda. 2004. Coactivation of Rac1 and Cdc42 at lamellipodia and membrane ruffles induced by epidermal growth factor. *Mol. Biol. Cell.* 15:1003–1010. doi:10.1091/mbc.E03-08-0609

L'Allemain, G., and J. Pouysségur. 1986. EGF and insulin action in fibroblasts. Evidence that phosphoinositide hydrolysis is not an essential mitogenic signalling pathway. *FEBS Lett.* 197:344–348. doi:10.1016/0014-5793(86)80354-4

L'Allemain, G., S. Paris, and J. Pouysségur. 1984. Growth factor action and intracellular pH regulation in fibroblasts. Evidence for a major role of the Na+/H+ antiport. *J. Biol. Chem.* 259:5809–5815.

L'Allemain, G., S. Paris, and J. Pouysségur. 1985. Role of a Na^+-dependent Cl^-/HCO_3^- exchange in regulation of intracellular pH in fibroblasts. *J. Biol. Chem.* 260:4877–4883.

Lagana, A., J. Vadnais, P.U. Le, T.N. Nguyen, R. Laprade, I.R. Nabi, and J. Noël. 2000. Regulation of the formation of tumor cell pseudopodia by the Na(+)/H(+) exchanger NHE1. *J. Cell Sci.* 113:3649–3662.

Lemmon, M.A., K.M. Ferguson, and C.S. Abrams. 2002. Pleckstrin homology domains and the cytoskeleton. *FEBS Lett.* 513:71–76. doi:10.1016/S0014-5793(01)03243-4

Liaw, Y.S., P.C. Yang, C.J. Yu, S.H. Kuo, K.T. Luh, Y.J. Lin, and M.L. Wu. 1998. PKC activation is required by EGF-stimulated Na(+)-H+ exchanger in human pleural mesothelial cells. *Am. J. Physiol.* 274:L665–L672.

Liberali, P., E. Kakkonen, G. Turacchio, C. Valente, A. Spaar, G. Perinetti, R.A. Böckmann, D. Corda, A. Colanzi, V. Marjomaki, and A. Luini. 2008. The closure of Pak1-dependent macropinosomes requires the phosphorylation of CtBP1/BARS. *EMBO J.* 27:970–981. doi:10.1038/emboj.2008.59

Lindmo, K., and H. Stenmark. 2006. Regulation of membrane traffic by phosphoinositide 3-kinases. *J. Cell Sci.* 119:605–614. doi:10.1242/jcs.02855

Liu, Y., and L.R. Rohrschneider. 2002. The gift of Gab. *FEBS Lett.* 515:1–7. doi:10.1016/S0014-5793(02)02425-0

Machacek, M., L. Hodgson, C. Welch, H. Elliott, O. Pertz, P. Nalbant, A. Abell, G.L. Johnson, K.M. Hahn, and G. Danuser. 2009. Coordination of Rho GTPase activities during cell protrusion. *Nature.* 461:99–103. doi:10.1038/nature08242

Makino, Y., M. Tsuda, S. Ichihara, T. Watanabe, M. Sakai, H. Sawa, K. Nagashima, S. Hatakeyama, and S. Tanaka. 2006. Elmo1 inhibits ubiquitylation of Dock180. *J. Cell Sci.* 119:923–932. doi:10.1242/jcs.02797

Marcoux, N., and K. Vuori. 2003. EGF receptor mediates adhesion-dependent activation of the Rac GTPase: a role for phosphatidylinositol 3-kinase and Vav2. *Oncogene.* 22:6100–6106. doi:10.1038/sj.onc.1206712

Masereel, B., L. Pochet, and D. Laeckmann. 2003. An overview of inhibitors of Na(+)/H(+) exchanger. *Eur. J. Med. Chem.* 38:547–554. doi:10.1016/S0223-5234(03)00100-4

Meier, O., K. Boucke, S.V. Hammer, S. Keller, R.P. Stidwill, S. Hemmi, and U.F. Greber. 2002. Adenovirus triggers macropinocytosis and endosomal leakage together with its clathrin-mediated uptake. *J. Cell Biol.* 158:1119–1131. doi:10.1083/jcb.200112067

Michiels, F., G.G. Habets, J.C. Stam, R.A. van der Kammen, and J.G. Collard. 1995. A role for Rac in Tiam1-induced membrane ruffling and invasion. *Nature.* 375:338–340. doi:10.1038/375338a0

Miesenböck, G., D.A. De Angelis, and J.E. Rothman. 1998. Visualizing secretion and synaptic transmission with pH-sensitive green fluorescent proteins. *Nature.* 394:192–195. doi:10.1038/28190

Moolenaar, W.H., R.Y. Tsien, P.T. van der Saag, and S.W. de Laat. 1983. Na+/H+ exchange and cytoplasmic pH in the action of growth factors in human fibroblasts. *Nature.* 304:645–648. doi:10.1038/304645a0

Mouneimne, G., L. Soon, V. DesMarais, M. Sidani, X. Song, S.C. Yip, M. Ghosh, R. Eddy, J.M. Backer, and J. Condeelis. 2004. Phospholipase C and

cofilin are required for carcinoma cell directionality in response to EGF stimulation. *J. Cell Biol.* 166:697–708. doi:10.1083/jcb.200405156

Nalbant, P., L. Hodgson, V. Kraynov, A. Toutchkine, and K.M. Hahn. 2004. Activation of endogenous Cdc42 visualized in living cells. *Science.* 305:1615–1619. doi:10.1126/science.1100367

Nguyen, A.W., and P.S. Daugherty. 2005. Evolutionary optimization of fluorescent proteins for intracellular FRET. *Nat. Biotechnol.* 23:355–360. doi:10.1038/nbt1066

Orlowski, J., and S. Grinstein. 2004. Diversity of the mammalian sodium/proton exchanger SLC9 gene family. *Pflugers Arch.* 447:549–565. doi:10.1007/s00424-003-1110-3

Pertz, O., L. Hodgson, R.L. Klemke, and K.M. Hahn. 2006. Spatiotemporal dynamics of RhoA activity in migrating cells. *Nature.* 440:1069–1072. doi:10.1038/nature04665

Racoosin, E.L., and J.A. Swanson. 1989. Macrophage colony-stimulating factor (rM-CSF) stimulates pinocytosis in bone marrow-derived macrophages. *J. Exp. Med.* 170:1635–1648. doi:10.1084/jem.170.5.1635

Ray, R.M., R.J. Vaidya, and L.R. Johnson. 2007. MEK/ERK regulates adherens junctions and migration through Rac1. *Cell Motil. Cytoskeleton.* 64:143–156. doi:10.1002/cm.20172

Ridley, A.J. 2006. Rho GTPases and actin dynamics in membrane protrusions and vesicle trafficking. *Trends Cell Biol.* 16:522–529. doi:10.1016/j.tcb.2006.08.006

Rothenberg, P., L. Glaser, P. Schlesinger, and D. Cassel. 1983. Activation of Na+/H+ exchange by epidermal growth factor elevates intracellular pH in A431 cells. *J. Biol. Chem.* 258:12644–12653.

Rupper, A., K. Lee, D. Knecht, and J. Cardelli. 2001. Sequential activities of phosphoinositide 3-kinase, PKB/Aakt, and Rab7 during macropinosome formation in *Dictyostelium*. *Mol. Biol. Cell.* 12:2813–2824.

Sallusto, F., M. Cella, C. Danieli, and A. Lanzavecchia. 1995. Dendritic cells use macropinocytosis and the mannose receptor to concentrate macromolecules in the major histocompatibility complex class II compartment: downregulation by cytokines and bacterial products. *J. Exp. Med.* 182:389–400. doi:10.1084/jem.182.2.389

Sandvig, K., S. Olsnes, O.W. Petersen, and B. van Deurs. 1987. Acidification of the cytosol inhibits endocytosis from coated pits. *J. Cell Biol.* 105:679–689. doi:10.1083/jcb.105.2.679

Sankaranarayanan, S., D. De Angelis, J.E. Rothman, and T.A. Ryan. 2000. The use of pHluorins for optical measurements of presynaptic activity. *Biophys. J.* 79:2199–2208. doi:10.1016/S0006-3495(00)76468-X

Seth, A., T. Otomo, H.L. Yin, and M.K. Rosen. 2003. Rational design of genetically encoded fluorescence resonance energy transfer-based sensors of cellular Cdc42 signaling. *Biochemistry.* 42:3997–4008. doi:10.1021/bi026881z

Shu, X., N.C. Shaner, C.A. Yarbrough, R.Y. Tsien, and S.J. Remington. 2006. Novel chromophores and buried charges control color in mFruits. *Biochemistry.* 45:9639–9647. doi:10.1021/bi060773l

Song, G., G. Ouyang, and S. Bao. 2005. The activation of Akt/PKB signaling pathway and cell survival. *J. Cell. Mol. Med.* 9:59–71. doi:10.1111/j.1582-4934.2005.tb00337.x

Song, X., X. Chen, H. Yamaguchi, G. Mouneimne, J.S. Condeelis, and R.J. Eddy. 2006. Initiation of cofilin activity in response to EGF is uncoupled from cofilin phosphorylation and dephosphorylation in carcinoma cells. *J. Cell Sci.* 119:2871–2881. doi:10.1242/jcs.03017

Srinivasan, S., F. Wang, S. Glavas, A. Ott, F. Hofmann, K. Aktories, D. Kalman, and H.R. Bourne. 2003. Rac and Cdc42 play distinct roles in regulating PI(3,4,5)P3 and polarity during neutrophil chemotaxis. *J. Cell Biol.* 160:375–385. doi:10.1083/jcb.200208179

Steinberg, B.E., and S. Grinstein. 2007. Assessment of phagosome formation and maturation by fluorescence microscopy. *Methods Mol. Biol.* 412:289–300. doi:10.1007/978-1-59745-467-4_19

Stock, C., B. Gassner, C.R. Hauck, H. Arnold, S. Mally, J.A. Eble, P. Dieterich, and A. Schwab. 2005. Migration of human melanoma cells depends on extracellular pH and Na+/H+ exchange. *J. Physiol.* 567:225–238. doi:10.1113/jphysiol.2005.088344

Swanson, J.A. 2008. Shaping cups into phagosomes and macropinosomes. *Nat. Rev. Mol. Cell Biol.* 9:639–649. doi:10.1038/nrm2447

Tamás, P., Z. Solti, P. Bauer, A. Illés, S. Sipeki, A. Bauer, A. Faragó, J. Downward, and L. Buday. 2003. Mechanism of epidermal growth factor regulation of Vav2, a guanine nucleotide exchange factor for Rac. *J. Biol. Chem.* 278:5163–5171. doi:10.1074/jbc.M207555200

Thomas, J.A., R.N. Buchsbaum, A. Zimniak, and E. Racker. 1979. Intracellular pH measurements in Ehrlich ascites tumor cells utilizing spectroscopic probes generated in situ. *Biochemistry.* 18:2210–2218. doi:10.1021/bi00578a012

Tzima, E., W.B. Kiosses, M.A. del Pozo, and M.A. Schwartz. 2003. Localized cdc42 activation, detected using a novel assay, mediates microtubule organizing center positioning in endothelial cells in response to fluid shear stress. *J. Biol. Chem.* 278:31020–31023. doi:10.1074/jbc.M301179200

Van Obberghen-Schilling, E., J.C. Chambard, S. Paris, G. L'Allemain, and J. Pouysségur. 1985. alpha-Thrombin-induced early mitogenic signalling events and G0 to S-phase transition of fibroblasts require continual external stimulation. *EMBO J.* 4:2927–2932.

van Rheenen, J., X. Song, W. van Roosmalen, M. Cammer, X. Chen, V. Desmarais, S.C. Yip, J.M. Backer, R.J. Eddy, and J.S. Condeelis. 2007. EGF-induced PIP2 hydrolysis releases and activates cofilin locally in carcinoma cells. *J. Cell Biol.* 179:1247–1259. doi:10.1083/jcb.200706206

Várnai, P., and T. Balla. 2008. Live cell imaging of phosphoinositides with expressed inositide binding protein domains. *Methods.* 46:167–176. doi:10.1016/j.ymeth.2008.09.019

Veithen, A., P. Cupers, P. Baudhuin, and P.J. Courtoy. 1996. v-Src induces constitutive macropinocytosis in rat fibroblasts. *J. Cell Sci.* 109:2005–2012.

West, M.A., M.S. Bretscher, and C. Watts. 1989. Distinct endocytotic pathways in epidermal growth factor-stimulated human carcinoma A431 cells. *J. Cell Biol.* 109:2731–2739. doi:10.1083/jcb.109.6.2731

West, M.A., A.R. Prescott, E.L. Eskelinen, A.J. Ridley, and C. Watts. 2000. Rac is required for constitutive macropinocytosis by dendritic cells but does not control its downregulation. *Curr. Biol.* 10:839–848. doi:10.1016/S0960-9822(00)00595-9

Yanaka, A., H. Suzuki, T. Shibahara, H. Matsui, A. Nakahara, and N. Tanaka. 2002. EGF promotes gastric mucosal restitution by activating Na(+)/H(+) exchange of epithelial cells. *Am. J. Physiol. Gastrointest. Liver Physiol.* 282:G866–G876.

Yeung, T., M. Terebiznik, L. Yu, J. Silvius, W.M. Abidi, M. Philips, T. Levine, A. Kapus, and S. Grinstein. 2006. Receptor activation alters inner surface potential during phagocytosis. *Science.* 313:347–351. doi:10.1126/science.1129551

Yeung, T., G.E. Gilbert, J. Shi, J. Silvius, A. Kapus, and S. Grinstein. 2008. Membrane phosphatidylserine regulates surface charge and protein localization. *Science.* 319:210–213. doi:10.1126/science.1152066